

# Accurate Structural Data Demystify B<sub>12</sub>: High-Resolution Solid-State Structure of Aquocobalamin Perchlorate and Structure Analysis of the Aquocobalamin Ion in Solution<sup>1</sup>

Christoph Kratky,<sup>\*,†</sup> Gerald Färber,<sup>†</sup> Karl Gruber,<sup>†</sup> Keith Wilson,<sup>§</sup>  
Zbigniew Dauter,<sup>§</sup> Hans-Friedrich Nolting,<sup>§</sup> Robert Konrat,<sup>||</sup> and  
Bernhard Kräutler<sup>\*,‡,||</sup>

Contribution from the Institut für Physikalische Chemie, Universität Graz, Heinrichstrasse 28, A-8010 Graz, Austria, European Molecular Biology Laboratory (EMBL), Outstation Hamburg, Notkestrasse 85, D-22603 Hamburg, Germany, Laboratory of Organic Chemistry of Eidgenössische Technische Hochschule (ETH), Universitätsstrasse 16, CH-8092 Zürich, Switzerland, and Institut für Organische Chemie, Universität Innsbruck, Innrain 52a, A-6020 Innsbruck, Austria

Received December 29, 1994<sup>®</sup>

**Abstract:** Experiments are described to elucidate the structure and solvation of aquocobalamin (vitamin B<sub>12a</sub>, 1<sup>+</sup>) in the crystal and in aqueous solution. Aquocobalamin (1<sup>+</sup>) is the B<sub>12</sub> derivative in which a water molecule replaces the axially coordinating organic substituent (methyl or 5'-desoxyadenosyl) at the  $\beta$ -side of the cobalt of the B<sub>12</sub> coenzymes. (1) A single-crystal structure analysis of aquocobalamin perchlorate (1<sup>+</sup>ClO<sub>4</sub><sup>-</sup>), using synchrotron radiation in combination with an imaging plate detector, yielded the most accurate structural data ever determined for a B<sub>12</sub> molecule. 1<sup>+</sup>ClO<sub>4</sub><sup>-</sup> crystallizes in the orthorhombic space group P2<sub>1</sub>2<sub>1</sub>2<sub>1</sub>,  $a = 15.042(11)$  Å,  $b = 23.715(14)$  Å,  $c = 25.104(12)$  Å, with four 1<sup>+</sup>ClO<sub>4</sub><sup>-</sup> moieties plus about 100 solvent water molecules per unit cell; 22 867 independent and 20 942 significant intensity data were recorded to a nominal resolution of 0.8 Å, and refinement against  $F^2$  quantities led to a conventional  $R$ -value of 0.050 for all 22 867 observations and to a structural model with an average ESD for all carbon–carbon bonds of 0.003 Å. In the crystal, the aquocobalamin ion has a very short axial bond between cobalt and the dimethylbenzimidazole (DMB) base of 1.925 (0.002) Å, which is rationalized as resulting from the very weak trans axial donor (water). Steric repulsion between the DMB base and the corrin ring induced by this short Co–DMB bond leads to a relatively large “butterfly” deformation with an “upward” fold angle of 18.71(0.07)°. The relevance of this observation for the “upward conformational deformation” hypothesis for the initiation of Co–C bond homolysis in coenzyme B<sub>12</sub> dependent enzymes is discussed. (2) EXAFS spectra were taken from an authentic sample of the aquocobalamin perchlorate crystals used for the X-ray structure analysis, as well as from 1<sup>+</sup>ClO<sub>4</sub><sup>-</sup> dissolved in a 1:1 mixture of water/ethylene glycol. Absorption spectra were recorded at 20 K between 7300 and 8700 eV, and the  $k^3$ -weighted EXAFS was extracted for a  $k$ -value between 2.7 and 14.4 Å<sup>-1</sup>. EXAFS spectra for solid and dissolved 1<sup>+</sup>ClO<sub>4</sub><sup>-</sup> agree closely, establishing identical cobalt coordination for the aquocobalamin ion in solution and in the solid state. A curve-fitting analysis on the Fourier filtered first-shell data yields a coordination number of 6 and an average distance of 1.90 Å for both samples. There is no evidence for a longer Co–N distance. This refutes data published by Sagi and Chance (*J. Am. Chem. Soc.* 1992, 114, 8061). (3) NMR experiments are described, constituting the first detailed NMR investigations on a B<sub>12</sub> derivative in H<sub>2</sub>O, including 2D homo- and heteronuclear studies on aquocobalamin chloride (1<sup>+</sup>Cl<sup>-</sup>) and assignment of signals due to the exchangeable amide protons of all nitrogens as well as measurements of amide proton exchange rates. The NMR data confirm the occupation of the axial coordination site at the Co(III) center by water, as well as the occurrence in solution of an intramolecular hydrogen bond to the axially coordinating water molecule, as observed in the crystal structure of 1<sup>+</sup>ClO<sub>4</sub><sup>-</sup>. However, significant differences of the structure of 1<sup>+</sup> in crystals of 1<sup>+</sup>ClO<sub>4</sub><sup>-</sup> and of 1<sup>+</sup> in aqueous solution are indicated from NOE data concerning the time-averaged conformation of the hydrogen-bonding *c*-acetamide side chain.

## Introduction

B<sub>12</sub> (Figure 1) has given rise to many mysteries concerning its structure, function, and reactivity. Both the unparalleled structural complexity and the observation of an organometallic cobalt–carbon bond in the B<sub>12</sub> coenzymes with their associated unique homolytic and heterolytic reactivities came as a complete surprise when discovered more than 30 years ago and have

remained disturbing and puzzling ever since. On the one hand, B<sub>12</sub> has attracted the curiosity of some of the most distinguished chemists of our century;<sup>2</sup> on the other hand, there is hardly any biologically relevant molecule which has provoked so many speculations about the mechanism of its function, some of them lacking either experimental support or chemical plausibility.

From the very beginning of the discovery of B<sub>12</sub>, X-ray crystal structure analysis has played a crucial role in the elucidation of its constitution, configuration, and conformation. Structural

<sup>†</sup> Universität Graz.

<sup>§</sup> EMBL Hamburg.

<sup>‡</sup> ETH.

<sup>||</sup> Universität Innsbruck.

<sup>®</sup> Abstract published in *Advance ACS Abstracts*, April 1, 1995.

(1) Coenzyme B<sub>12</sub> Chemistry, Part 4. For Part 3, see ref 7.

(2) See, e.g., the chapters by Hodgkin, D. C.; Woodward, R. B.; Eschenmoser, A.; et al. In *Vitamin B<sub>12</sub>*; Zagalak, B., Friedrich, W., Eds.; Walter de Gruyter: Berlin, New York, 1979.

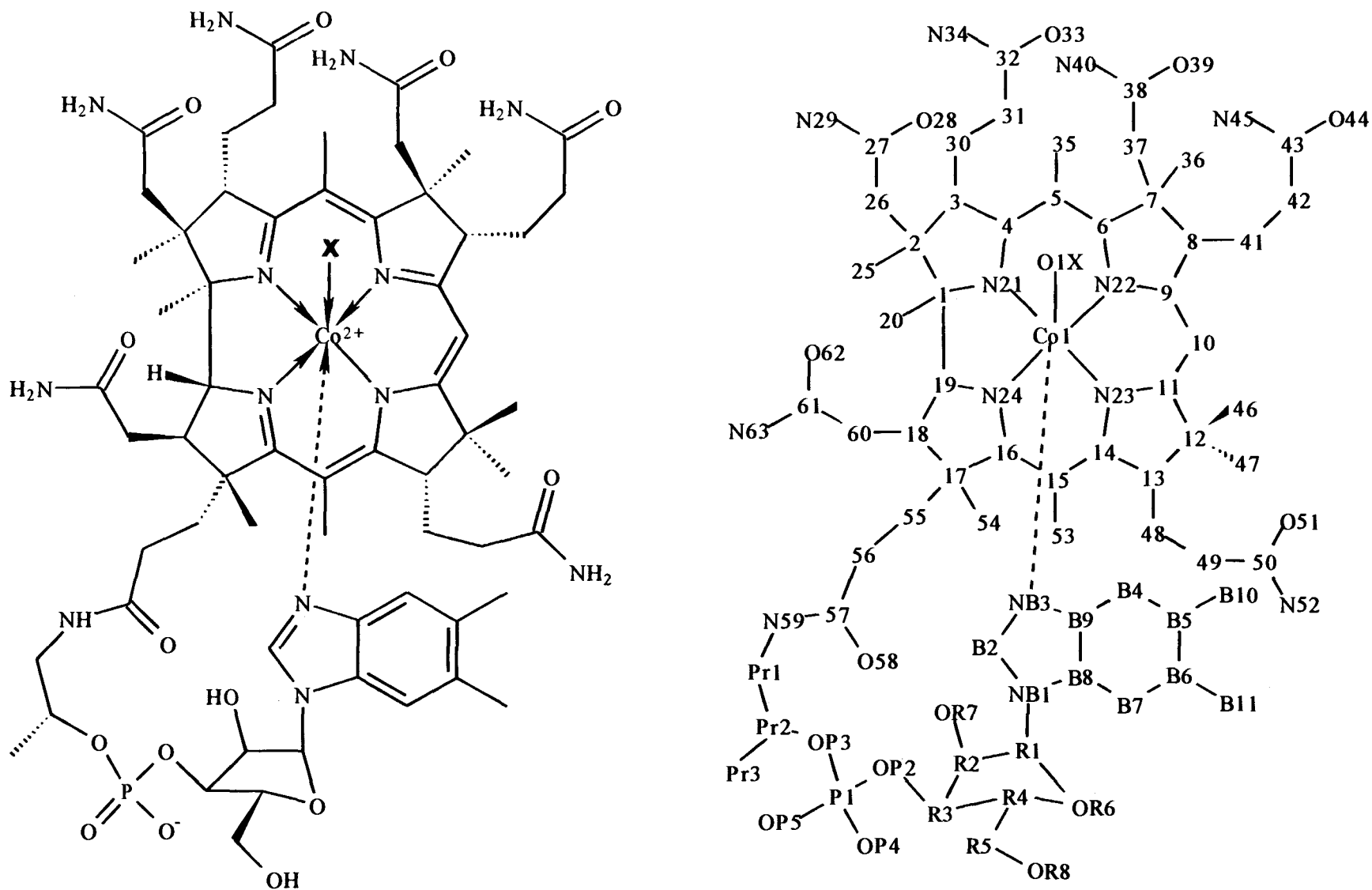


**Figure 1.** Left: structural formulae of cobalamins 1<sup>+</sup> (aquocobalamin) (X = H<sub>2</sub>O), 2 (vitamin B<sub>12</sub>) (X = CN<sup>-</sup>), 3 (coenzyme B<sub>12</sub>) (X = 5'-desoxyadenosyl<sup>-</sup>), 4 (methylcobalamin) (X = CH<sub>3</sub><sup>-</sup>), 5 (hydroxocobalamin) (X = OH<sup>-</sup>), and 6 (cob(II)alamin B<sub>12r</sub>) (X = e<sup>-</sup>). Right: atom-numbering system used for the description of X-ray and NMR results on the aquocobalamin ion (1<sup>+</sup>).

results from the solid state have more or less tacitly been assumed as representative for the solution structure of B<sub>12</sub>, an assumption which was corroborated (at least with respect to one of possibly several solution conformations) whenever challenged by NMR studies on B<sub>12</sub> derivatives of known crystal structure.<sup>3,4h,k</sup> In recent years, several reports have appeared describing structural studies on B<sub>12</sub> derivatives in solution using EXAFS spectroscopy.<sup>5</sup> While some of these results agreed very well with previously determined crystal structures (e.g., coenzyme B<sub>12</sub>,<sup>5a,b</sup> methylcobalamin<sup>5a</sup>), others either disagreed with crystallographic evidence (B<sub>12r</sub>,<sup>5b</sup> vitamin B<sub>12</sub>)<sup>5a</sup> or were at variance with expectations from coordination chemistry. The disagreement mainly concerned the length of the axial Co–N bond, and it was either blamed on the fact that the crystallographic data were “old” (referring to Dorothy Hodgkin’s vitamin B<sub>12</sub> data,<sup>6,4a</sup> which were later shown to be essentially correct)<sup>7</sup> or implicitly ascribed to differences between the solid-state and solution structures (in the case of B<sub>12r</sub>).<sup>5b</sup>

A particularly striking example is the EXAFS-based structure analysis of “aquocobalamin”, the B<sub>12</sub> species with a water molecule replacing the organic ligand (methyl or deoxyadenosyl) of the B<sub>12</sub> coenzymes. There, chemical plausibility and evidence from model complexes predict a short axial Co–N distance as a result of the weak donor ability of the trans-configured aquo ligand. The EXAFS experiment reported by Sagi and Chance<sup>5a</sup> yielded a distance of 2.14 Å, almost as long as the axial Co–N distance observed in crystal structures of alkylcobalamins and much longer than the distance observed in vitamin B<sub>12</sub>, where the trans ligand is a (better donating) cyano group. The explanation provided for the “unexpected” long axial Co–N distance was steric repulsion between the 5,6-dimethylbenzimidazole (DMB) base and the equatorial corrin ligand.<sup>5a</sup> EXAFS spectroscopy<sup>8</sup> is believed to be capable of determining metal–ligand distances with the precision and accuracy of small-molecule crystallography,<sup>5a</sup> and indeed the reported Co–N distance was accompanied by an estimated least-squares standard deviation of 0.03 Å, putting the result at about the same level of statistical significance as the hitherto available crystallographic evidence on B<sub>12</sub>.

Recently, Calafat and Marzilli<sup>9</sup> reported an NMR investigation of “nonalkyl” cobalamins including aquocobalamin acetate (1<sup>+</sup>Ac<sup>-</sup>), leading to the indirect conclusion that the Sagi and Chance result on aquocobalamin is unlikely to be correct. A similar conclusion emerged from a study (NMR spectroscopic and X-ray crystallographic) from our laboratories, involving vitamin B<sub>12</sub> (2) and Co-β-cyanoimidazolylcobamide, the derivative with imidazole replacing DMB.<sup>7</sup> However, both studies relied on indirect evidence from model complexes<sup>9</sup> or were based on solid-state crystallographic data from cobalamins.<sup>7</sup> Thus, while each of these studies makes the Sagi and Chance results on aquocobalamin and vitamin B<sub>12</sub> more implausible, none could conclusively disprove it. Resolution of this matter appeared highly desirable, also in order to assess other published EXAFS results,<sup>5</sup> which are as yet not paralleled by single-crystal diffraction data,<sup>5c–g</sup> including results on B<sub>12</sub> dependent enzymes.<sup>5f,g</sup>

Therefore, we decided on a concerted effort toward elucidating the structure of the aquo-B<sub>12</sub> system with the two established techniques for high-resolution structure analysis (X-ray crystal structure analysis, NMR spectroscopy) and with EXAFS spectroscopy, employing advanced technology. It is believed that this should equally contribute to the understanding of B<sub>12</sub> chemistry and provide an assessment for the applicability of EXAFS spectroscopy to problems of high-resolution structure determination. Our aim was to consolidate the structural data on B<sub>12</sub> with chemistry’s solid foundations,<sup>10</sup> supported by numerous investigations of B<sub>12</sub> model complexes.<sup>11</sup>

Historically, aquocobalamin (1<sup>+</sup>) (or hydroxocobalamin, 5) was the second corrinoid isolated from biological sources (following the isolation of cyanocobalamin, 2), and it was originally termed vitamin B<sub>12a</sub>.<sup>12,13</sup> The interest in the structure of “nonalkyl” cobalamins has recently been revived by Calafat and Marzilli.<sup>9</sup> There is a well-known correlation between the strength of the coordination of the nucleotide base and the nature of the β-ligand in cobalamins, which shows up in a dependence of the pK<sub>a</sub> value of the protonation of the DMB base on the nature of the β-ligand.<sup>14</sup> This puts aquocobalamin at the extreme of low pK (pK<sub>a</sub> ≈ -2.1),<sup>14</sup> corroborating the fact that it is a cobalamin with an extremely weak donor on the β-side. Therefore, knowledge of the structure of 1<sup>+</sup> is indispensable for assessing the effect of the donor ability of the β-ligand on the rest of the B<sub>12</sub> molecule, since the structure of 1<sup>+</sup> is bound to be an “extreme” in one way or another. Mechanical deformations of the corrin ring (“upward conformational distortion”)<sup>15</sup> are believed to play a key role in the biological function of coenzyme B<sub>12</sub> (3) by assisting homolysis of the cobalt–carbon bond.

The present communication describes three sets of experiments on aquocobalamin (1<sup>+</sup>) with chloride or perchlorate as counterions: (1) a crystal structure analysis of 1<sup>+</sup>ClO<sub>4</sub><sup>-</sup>, em-

(3) Bax, A.; Marzilli, L. G.; Summers, M. F. *J. Am. Chem. Soc.* **1987**, *109*, 566.

(4) (a) Brink-Shoemaker, C.; Cruickshank, D. W. J.; Hodgkin, D. C.; Kamper, M. J.; Pilling, D. *Proc. R. Soc. London, Ser. A* **1964**, *278*, 1. (b) Lenhart, P. G. *Proc. R. Soc. London, Ser. A* **1968**, *303*, 45. (c) Hawkinson, S. W.; Coulter, C. L.; Greaves, M. L. *Proc. R. Soc. London, Ser. A* **1970**, *318*, 143. (d) Stoeckli-Evans, H.; Edmond, E.; Hodgkin, D. C. *J. Chem. Soc., Perkin Trans. 2* **1972**, 605. (e) Kopf, J.; van Deuten, K.; Bieganski, R.; Friedrich, W. Z. *Naturforsch.* **1981**, *C36*, 506. (f) Waters, J. M.; Waters, T. N. M. *Proc. Indian Acad. Sci., Chem. Sci.* **1984**, *93*, 219. (g) Alcock, N. W.; Dixon, R. M.; Golding, B. T. *J. Chem. Soc., Chem. Commun.* **1985**, 603. (h) Rossi, M.; Glusker, J. P.; Randaccio, L.; Summers, M. F.; Toscano, P. J.; Marzilli, L. G. *J. Am. Chem. Soc.* **1985**, *107*, 1729. (i) Savage, H. F. J.; Lindlev, P. F.; Finney, J. L.; Timmins, P. A. *Acta Crystallogr. B* **1987**, *43*, 280. (j) Kräutler, B.; Keller, W.; Kratky, C. *J. Am. Chem. Soc.* **1989**, *111*, 8936. (k) Pagano, T. P.; Marzilli, L. G.; Flocco, M. M.; Tsai, C.; Carrell, H. L.; Glusker, J. P. *J. Am. Chem. Soc.* **1991**, *113*, 531. (l) Hohenester, E.; Kratky, C.; Kräutler, B. *J. Am. Chem. Soc.* **1991**, *113*, 4523. (m) Brown, K. N.; Zou, X.; Wu, G.-Z.; Zubkowski, J. D.; Valente, E. J. *Inorg. Chem.* **1994**, in press.

(5) (a) Sagi, I.; Chance, M. R. *J. Am. Chem. Soc.* **1992**, *114*, 8061. (b) Sagi, I.; Wirt, M. D.; Chen, E.; Frisbie, S.; Chance, M. R. *J. Am. Chem. Soc.* **1990**, *112*, 8639. (c) Wirt, M. D.; Sagi, I.; Chen, E.; Frisbie, S. M.; Lee, R.; Chance, M. R. *J. Am. Chem. Soc.* **1991**, *113*, 5299. (d) Wirt, M. D.; Sagi, I.; Chance, M. R. *Biophys. J.* **1992**, *63*, 412. (e) Wirt, M. D.; Chance, M. R. *J. Inorg. Biochem.* **1993**, *49*, 265. (f) Wirt, M. D.; Chance, M. R.; Retey, J. *FASEB J.* **1992**, *6*, A335. (g) Wirt, M. D.; Chance, M. R.; Retey, J. *Biophys. J.* **1993**, *64*, A369.

(6) Hodgkin, D. C.; Lindsey, J.; Sparks, R. A.; Trueblood, K. N.; White, J. G. *Proc. R. Soc. London, Ser. A* **1962**, *266*, 494.

(7) Kräutler, B.; Konrat, R.; Stupperich, E.; Färber, G.; Gruber, K.; Kratky, C. *Inorg. Chem.* **1994**, *33*, 4128.

(8) Bertagnolli, H.; Ertel, T. S. *Angew. Chem.* **1994**, *106*, 15.

(9) Calafat, M.; Marzilli, L. G. *J. Am. Chem. Soc.* **1993**, *115*, 9182.

(10) Pratt, J. M. *Inorganic Chemistry of Vitamin B<sub>12</sub>*; Academic Press: London, New York, 1972.

(11) See, e.g., the following reviews: (a) Bresciani-Pahor, N.; Forcolin, M.; Marzilli, L. G.; Randaccio, L.; Summers, M. F.; Toscano, P. J. *Coord. Chem. Rev.* **1985**, *63*, 1. (b) Randaccio, L.; Bresciani-Pahor, N.; Zangrando, E.; Marzilli, L. G. *Chem. Soc. Rev.* **1989**, *18*, 225.

(12) Kaczka, E.; Wolf, D. E.; Folkers, U. *J. Am. Chem. Soc.* **1949**, *71*, 1514.

(13) For reviews on the B<sub>12</sub> chemistry, see: (a) Friedrich, W. *Vitamins*; Walter de Gruyter: Berlin, New York, 1988. (b) Isler, O.; Brubacher, G.; Ghisler, S.; Kräutler, B. *Vitamine II*; Georg Thieme Verlag: Stuttgart, New York, 1988; pp 340–388. (c) Pratt, J. M. In *Metal Ions in Biological Systems*; Siegel, H., Siegel, A., Eds.; Marcel Dekker, Inc.: New York, Basel, Hong Kong, 1993; p 229.

(14) Aquocobalamin (1<sup>+</sup>), pK<sub>a</sub> = -2.1; vitamin B<sub>12</sub> (2), pK<sub>a</sub> = 0.1; methylcobalamin (4), pK<sub>a</sub> = 2.9; coenzyme B<sub>12</sub> (3), pK<sub>a</sub> = 3.7 (data from Brown, K. L.; Hakimi, J. M. *J. Am. Chem. Soc.* **1984**, *106*, 7894).

playing synchrotron radiation and imaging plate detector technology, constituting by far the most accurate structure determination of a B<sub>12</sub> ever reported, and yielding a molecular description with the precision and reliability of a very good small-molecule structure; (2) EXAFS measurements on crystals of the same batch used for the crystal structure analysis, as well as on solutions of 1<sup>+</sup>ClO<sub>4</sub><sup>-</sup>, permitting a correlation between the solution spectra and the spectra from crystals of accurately known structure; and (3) the first detailed NMR investigations on a B<sub>12</sub> derivative in H<sub>2</sub>O, in particular of solutions of 1<sup>+</sup>Cl<sup>-</sup>, including 2D homo- and heteronuclear studies and assignment of signals due to the exchangeable amide protons of all nitrogens as well as measurements of amide proton exchange rates. These studies confirm the occupation of the axial coordination site at the Co(III) center by water, as well as the occurrence in solution of an intramolecular hydrogen bond to the axially coordinating water molecule, as observed in the crystal structure of 1<sup>+</sup>ClO<sub>4</sub><sup>-</sup>. In addition, the recently reported<sup>9</sup> assignment for 1<sup>+</sup>Ac<sup>-</sup> was verified.

## Results

**Single-Crystal Structure Analysis of Aquocobalamin Perchlorate (1<sup>+</sup>ClO<sub>4</sub><sup>-</sup>).** Crystals were grown from water after exchanging the chloride counterion of commercially available "aquocobalamin hydrochloride" by perchlorate.<sup>17</sup> We were not able to obtain suitable crystals from water-acetone. Cell dimensions were determined at ambient temperature<sup>18</sup> on a conventional four-circle diffractometer; intensity data (from the same crystal) were obtained with synchrotron radiation ( $\lambda = 0.65 \text{ \AA}$ ) using a rotation camera with imaging plate detector. Since the cell dimensions refined against the imaging plate synchrotron data correlate strongly with the wavelength and the crystal-detector distance, they were regarded less reliable than the lattice constants obtained with the diffractometer.<sup>19</sup>

The crystal structure was refined against a total of 22 867 reflections (Friedel equivalents not merged) with a maximum

(15) This concept has originally obtained early experimental support through work by Schrauzer<sup>16a</sup> and Pratt,<sup>16f</sup> who referred to the "mechanicochemical" nature of steric factors governing Co-C bond cleavage. It has subsequently been advanced under a variety of names—butterfly-bending,<sup>16a</sup> upward conformational distortion,<sup>16d</sup> corrin butterfly conformational distortion,<sup>16c</sup> and conformational trigger mechanism<sup>16e</sup>—by several of the leading scientists in the B<sub>12</sub> field, including Halpern,<sup>41a</sup> Marzilli,<sup>16b</sup> Glusker,<sup>20</sup> Golding,<sup>16c</sup> and Finke,<sup>16c</sup>; see, however, the critical statements by Brown et al.<sup>16g</sup> and Krättiler et al.<sup>41</sup>

(16) (a) Schrauzer, G. N.; Grate, J. H.; Hashimoto, M.; Maihub, A. In *Vitamin B<sub>12</sub>, Proceedings of the Third European Conference*; Zagalak, B., Friedrich, W., Eds.; W de Gruyter: Berlin, 1979; p 511. (b) Marzilli, L. G. In *Bioinorganic Catalysis*; Reedijk, J., Ed.; Marcel Dekker, Inc.: New York, 1993; p 227. (c) Waddington, M. D.; Finke, R. G. *J. Am. Chem. Soc.* **1993**, *115*, 4629. (d) Halpern, J. *Science* **1985**, *227*, 869. (e) Golding, B. T.; Rao, D. N. R. In *Enzyme Mechanisms*; Page, M. I.; Williams, A., Eds.; Royal Society of Chemistry: London, 1987; p 404. (f) Chemaly, S. M.; Pratt, J. M. *J. Chem. Soc., Dalton Trans.* **1980**, 2274. (g) Brown, K. L.; Brooks, H. B. *Inorg. Chem.* **1991**, *30*, 3420.

(17) Crystallization of "aquocobalamin hydrochloride" from water/acetone leads to the formation of chlorocobalamin crystals. Its crystal structure has (accidentally) been determined in the course of the present investigation.<sup>19b</sup> The result of this structure analysis will be reported elsewhere.

(18) We also tried to cool the crystals grown from water to cryotemperature ( $\approx 100 \text{ K}$ ). Although the crystals showed similar cell dimensions at low temperature, the cooling resulted in a deterioration of the diffraction pattern (increase of the mosaic spread), which compelled us to carry on at room temperature, where they exhibit favorable mosaicity and excellent stability in the X-ray beam, permitting the collection of several diffraction data sets from the same crystal.<sup>19</sup>

(19) (a) Following the data collection on the synchrotron, we also collected data on a rotating anode source with an imaging plate detector and on a sealed tube source with a conventional diffractometer, using the same crystal.<sup>19b</sup> By all standards, the synchrotron data were found to be superior to the other two data sets. A detailed comparison between the results of the three data collections will be given elsewhere. (b) Färber, G. Ph.D. Thesis, University of Graz, 1993.

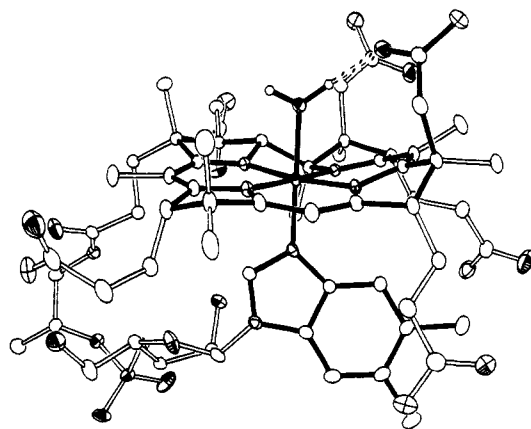


**Figure 2.** ORTEP-type representation<sup>80b</sup> of the 1<sup>+</sup> ion, as observed at room temperature in the crystal structure of 1<sup>+</sup>ClO<sub>4</sub><sup>-</sup>. Note that thermal ellipsoids are drawn at the 10% probability level (as opposed to the usual 50%) in order to obtain a less clustered picture. Carbon atoms are represented as open ellipsoids, and principal axes have been drawn for nitrogen and principal axes plus shaded octants for oxygen, phosphorus and cobalt. The intramolecular hydrogen bond between the coordinated water molecule and the carbonyl oxygen of the c-acetamide is represented as a dashed bond. Hydrogen atoms were omitted with the exception of the two hydrogens on the coordinated water molecule, which have been observed in a difference electron density map and were included in the crystallographic refinement.

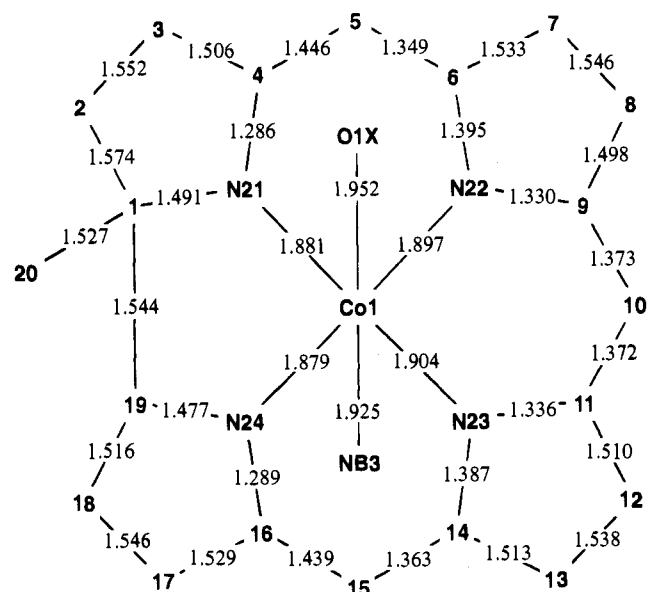


**Figure 3.** Bond lengths as observed in the crystal structure of 1<sup>+</sup>ClO<sub>4</sub><sup>-</sup>. The ESD's for C-C and C-N bonds are 0.003 Å and for Co-N and Co-O bonds 0.002 Å.

resolution of 0.8 Å. Refinement of 1165 parameters (subject to 649 restraints) converged at *R*-values of 0.045 for the 20 942 significant reflections and 0.050 for all 22 867 reflections. At the close of refinement, the average standard deviation for a carbon-carbon bond was 0.003 Å. Atomic coordinates are given in Table S2 (supplementary material). An ORTEP-type drawing of the aquocobalamin ion as observed in the crystal structure of 1<sup>+</sup>ClO<sub>4</sub><sup>-</sup> is shown in Figure 2. Selected bond lengths for the corrin ring and the cobalt coordination are given in Figure 3. The bonding distances of the conjugated system show the earlier noted<sup>20a</sup> symmetry about the Co-C10 line;

(20) (a) Glusker, J. P. In *B<sub>12</sub>*; Dolphin, D., Ed.; Wiley: New York, 1982; Vol. 1, p 23. (b) Rossi, M.; Glusker, J. P. In *Molecular Structure and Energetics*; Liebman, J. F., Greenberg, A., Eds.; VCH Publishers: Weinheim, FRG, 1988; Vol. X, p 1.

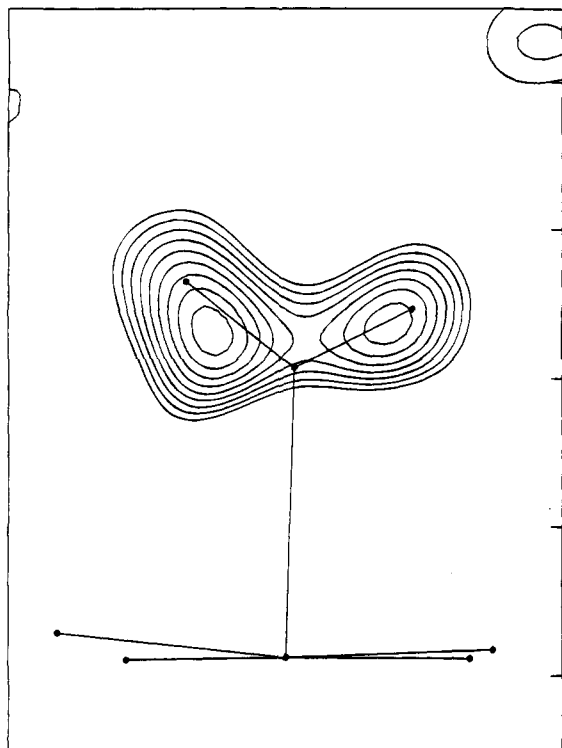


**Figure 4.** "Omit" map for the hydrogen atoms of the cobalt-coordinated water molecule in the crystal structure of  $1^+\text{ClO}_4^-$ . The figure shows the result of a  $\Delta F$  Fourier synthesis with the final coordinates, excluding the two protons. The hydrogen atom positions indicated in the figure were obtained by refining the H-coordinates subject to an O–H distance restraint of 0.95 Å; lowest contour  $0.1 e\text{\AA}^{-3}$ , increment  $0.02 e\text{\AA}^{-3}$ , rms deviation of electron density from the mean value  $0.06 e\text{\AA}^{-3}$ .

deviations from this symmetry are small but statistically significant ( $\chi^2 = 28$  for six degrees of freedom). These quantities agree remarkably well with theoretical values proposed more than 30 years ago<sup>21</sup> on the basis of very crude bond orders. A thermal motion analysis<sup>22</sup> for the corrin ring and its directly attached substituents yields bond length corrections of 0.001–0.002 Å.

The most noteworthy features of the crystal structure of  $1^+\text{ClO}_4^-$  are (1) the short axial Co–N(DMB) distance of 1.925 (0.002) Å, which is the shortest axial Co–N distance observed so far in a cobalamin; (2) the large upward folding angle<sup>23</sup> of 18.71(0.07)°; (3) the base tilt angle<sup>25</sup> of 5.46(9)°; (4) an intramolecular hydrogen bond between the cobalt-coordinated water molecule and the carbonyl oxygen atom of the *c*-acetamide (O39⋅⋅H1(O1x), 1.78 Å; O39⋅⋅O1x, 2.662 Å). A very similar intramolecular hydrogen bond has been observed in the only other crystal structure of a B<sub>12</sub> molecule with a water axially coordinating the metal center, i.e., for aquocyanocobyrinic acid,<sup>26</sup> and (5) direct observability in a difference Fourier synthesis of the electron density originating from the two protons of the cobalt-coordinated water molecule (Figure 4).

$1^+\text{ClO}_4^-$  crystallizes in the orthorhombic space group  $P2_12_12_1$  with four cobalamin units plus 100 solvent water

(21) Hodgkin, D. C. *Proc. R. Soc. London, Ser. A* **1962**, 288, 294.

(22) Dunitz, J. D.; Shoemaker, V.; Trueblood, K. N. *J. Phys. Chem.* **1988**, 92, 856.

(23) The upward folding angle is defined<sup>24</sup> as the dihedral angle between the planes through atoms N21, C4, C5, C6, N22, C9, C10 and C10, C11, N23, C14, C15, C16, N24, respectively (see Figure 1).

(24) Lenhart, P. G. *Proc. R. Soc. London, Ser. A* **1968**, 303, 45.

(25) The base tilt angle has been defined<sup>7</sup> as one-half the difference between the two axial Co–N–C angles, i.e.,  $(\phi_{\text{C}01-\text{N}03-\text{B}9} - \phi_{\text{C}01-\text{N}03-\text{B}2})/2$  (see Figure 1 for a definition of the atom numbering).

(26) Venkatesan, K.; Dale, D.; Hodgkin, D. C.; Nockolds, C. E.; Moore, F. H.; O'Connor, B. H. *Proc. R. Soc. London, Ser. A* **1971**, 323, 455.

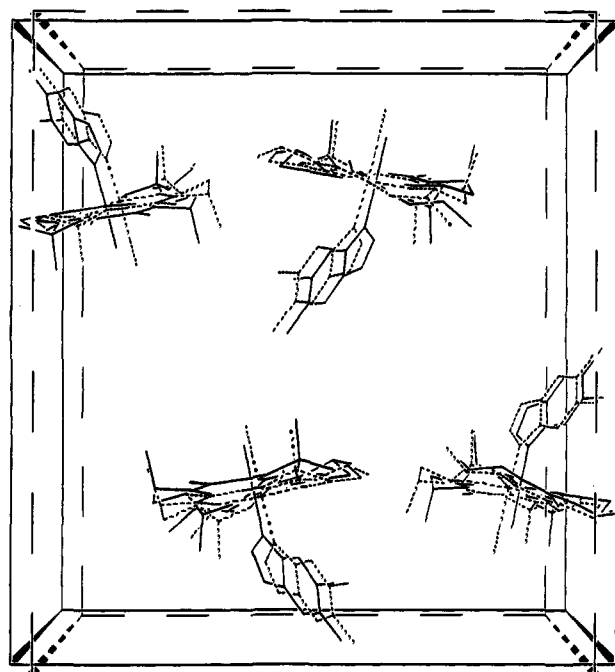


**Figure 5.** Superposition of the crystal structures of aquocobalamin perchlorate ( $1^+\text{ClO}_4^-$ ) (full lines) with vitamin B<sub>12</sub> (**2**) (dashed), projected down the crystallographic *a*-axis. Side chains and solvent molecules have been omitted for clarity.

molecules per unit cell. The B<sub>12</sub> molecules are packed into the orthorhombic  $P2_12_12_1$  unit cell in a way characteristic for the majority of other "complete corrinoids".<sup>4,7</sup> This preferred mode of packing can be exemplified by comparing the crystal structure of  $1^+\text{ClO}_4^-$  with that of the vitamin **2**.<sup>4a,7</sup> Figure 5 shows a superposition of the unit-cell content of the crystal structures of  $1^+\text{ClO}_4^-$  and **2**, projected down the crystallographic *a*-axis. Only the corrin rings and the two cobalt ligands are shown for each B<sub>12</sub> molecule to obtain a less cluttered picture. The structural similarity in the positions of the B<sub>12</sub> molecules in the unit cell also extends to part of the solvent domain, which shows the perchlorate counterion in the crystal structure of  $1^+\text{ClO}_4^-$  at the same position as the (only) acetone molecule in the structure of **2**. Also some—but by no means all—of the solvent water molecules are observed in similar positions in the two structures: 8 of the 25 solvent water molecules of the aquocobalamin structure are observed within 1 Å of one of the 12 fully occupied solvent sites in the vitamin structure. As a consequence, the hydrogen-bonding network is quite different between the two crystal structures, which is remarkable in view of the very similar packing of the cobalamin molecules. A listing of all intra- and intermolecular hydrogen bonds observed in the crystal structure of  $1^+\text{ClO}_4^-$  is given in Table S4 (supplementary material).

Figure 6 shows a superposition of the molecules of  $1^+\text{ClO}_4^-$  (full line) with **2** (dashed), as observed in their respective crystal structures. The similarity in the overall molecular conformation is in line with the above packing resemblance, although there are differences in the conformations of some of the side chains; particularly noteworthy is the difference in the conformation of the *c*-acetamide side chain, which—relative to **2**—swings around by almost 180° to form an intramolecular hydrogen bond to the Co-coordinated water molecule. Differences exceeding 1 Å between corresponding atoms are also observed for the *b*- and *g*-side chains and the ribose hydroxy group OR8. The latter group is found to be

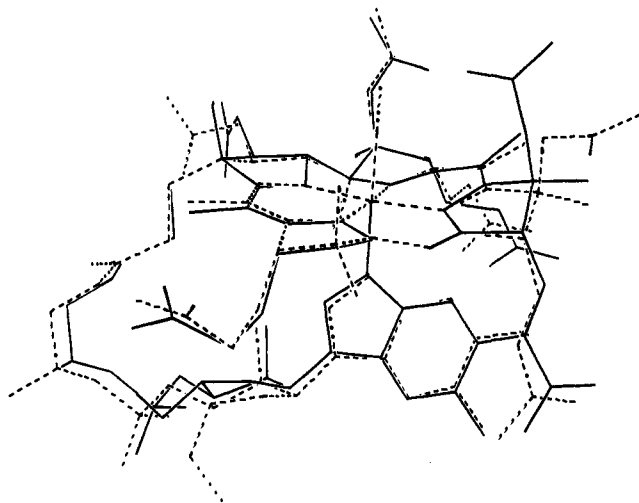


**Figure 6.** Superposition (N21, N22, N23, and N24) of the cobalamin molecules of  $1^+$  (solid line) and  $2$  (broken line), as observed in their respective crystal structures.

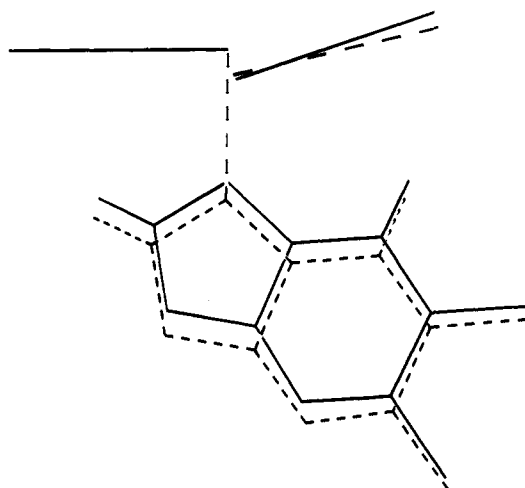


**Figure 7.** Conformational effects of shortening the axial Co–N bond in a cobalamin. The figure shows the result of a superposition of atoms C10, C11, N23, C14, C15, C16, and N24 of the crystal structures of aquocobalamin perchlorate ( $1^+\text{ClO}_4^-$ ) (full lines) and coenzyme B<sub>12</sub> ( $3$ ) (dashed lines).<sup>41</sup> Each molecule is represented by its nucleotide base, the axial Co–N bond, and the projection of the “northern” (N21, C4, C5, C6, N22, C9, C10) and “southern” (C10, C11, N23, C14, C15, C16, N24) least-squares planes.

disordered in the crystal structure of  $1^+\text{ClO}_4^-$ , where it is distributed over two positions with respective occupancies of 0.3 and 0.7.

**EXAFS Spectra of Aquocobalamin Perchlorate ( $1^+\text{ClO}_4^-$ ).** EXAFS spectra have been taken at 20 K for  $1^+\text{ClO}_4^-$  in water/ethylene glycol (1:1) and for a sample of crystalline  $1^+\text{ClO}_4^-$ . Crystals from the same crystallization batch were used for the X-ray structure determination and the solid-state absorption measurement, in order to relate the absorption spectra to the result of the crystal structure analysis with as few assumptions as possible. Owing to the good solubility, both spectra could be measured in absorption mode, with a reasonable jump at the cobalt absorption edge.<sup>27</sup> Absorption spectra were recorded between 7300 and 8700 eV, and the  $k^3$ -weighted EXAFS was extracted for a  $k$ -value between 2.7 and 14.4  $\text{\AA}^{-1}$ . The resulting spectra are given in Figures 8 (solution) and S7 (crystalline) (supplementary material). A

(27) Absorption values before/at/after the cobalt absorption edge for  $1^+\text{ClO}_4^-$ : solution, 1.81/2.17/2.01; crystal, 0.86/0.99/0.93.

superposition of the two EXAFS spectra of  $1^+\text{ClO}_4^-$  is shown in Figure 9. Compared to the previously reported EXAFS spectra of “aquocobalamin”,<sup>5a,28</sup> (Figure 8, dashed line), the used portion of our spectra extend to higher  $k$ -values (14.4 vs <12  $\text{\AA}^{-1}$ ). A comparison of the Fourier transforms of the  $k^3$ -weighted EXAFS spectra for dissolved and crystalline  $1^+\text{ClO}_4^-$  is shown in Figure 10.

**NMR Analysis of Aquocobalamin Chloride ( $1^+\text{Cl}^-$ ) in Aqueous Solution.** NMR experiments were performed at 26 °C with 10 mM solutions of  $1^+\text{Cl}^-$  in 90% H<sub>2</sub>O/10% D<sub>2</sub>O, buffered with 100 mM phosphate buffer in the pH range from 1.6 to 6.6,<sup>29</sup> as well as at pH 9.3 (where the conjugated base of  $1^+$  prevails, i.e.,  $5$ ). The signals of protons ( $^1\text{H}$ ), carbons ( $^{13}\text{C}$ ), and nitrogens ( $^{15}\text{N}$ ) were assigned for the spectra of solutions of  $1^+\text{Cl}^-$  at pH 3.5 (see Table 1). The signals of the nonexchangeable protons and the carbons of aquocobalamin acetate ( $1^+\text{Ac}^-$ ) and hydroxocobalamin ( $5$ ) have been assigned earlier by Calafat and Marzilli.<sup>9</sup> With the exception of the two diastereotopic protons at C48 (reported both at 2.03 ppm<sup>9</sup>), which we observed at 2.03 and 1.92 ppm in the spectrum of  $1^+\text{Cl}^-$  at pH 3.5, there were no significant differences between the two sets of data. To resolve residual ambiguities in the signal assignment of the carbons and protons of C55 and C56, we have performed a band-selective gradient-enhanced HMBC experiment.<sup>30</sup> This technique exploits the very high two-dimensional resolution obtained by selective excitation of the carbon spectral region of interest. The resulting spectrum given in Figure S8 (supplementary material) shows long range correlation ( $^3J_{\text{CH}}$ ) between the methyl protons of C54 and one of the two carbons in question, i.e., C55 which is located at 35.5 ppm. In addition, we have assigned the signals of the amide protons and the (directly bonded) amide nitrogens by virtue of the recently developed “watergate” ROESY<sup>31</sup> and  $^1\text{H}$ - $^{15}\text{N}$  PFG-HSQC<sup>32,33</sup> experiment. Figure 11 shows the NOEs between the amide protons and the high-field methylene protons. As an illustrative example, those cross peaks are depicted which were used for the assignment of the c-side chain amide protons. For each amide group, the low-field proton signal could be assigned to H<sub>E</sub> due to ROESY cross peaks.

Assignment of the four corrin ring nitrogens (N21, N22, N23, and N24) and the nitrogens in the benzimidazole base (NB1 and NB3) was achieved by using a  $^1\text{H}$ - $^{15}\text{N}$  PFG-HMBC<sup>32,34</sup> experiment. The various pyrrole nitrogens were identified by using long range correlation peaks to protons separated by two or three bonds. For example, the nitrogen N21 shows a long range correlation peak to the methyl group C20. The two nitrogens N22 (ring B) and N23 (ring C) both show correlations to H(C10), and could be discriminated by an additional long range peak of N22 to H(C8). N24 could reliably be assigned by the observation of a correlation to H(C19). Unfortunately, both nitrogens of the benzimidazole base only show long range correlations to H(B2). Thus, signal assignment was made by

(28) It is not evident from the data given in Sagi and Chance’s paper<sup>5a</sup> whether their EXAFS spectra were taken from aquo- or hydroxocobalamin.

(29) The equilibrium constant for ligand exchange between water and chloride ion is  $K = 1.3$ .<sup>10</sup> At the concentrations of  $1^+\text{Cl}^-$  used in the NMR experiments, the aquocobalamin ion ( $1^+$ ) is by far the predominant species in acidic aqueous solution;  $\text{p}K_a(1^+) = 7.6 \pm 0.2$ .<sup>10</sup>

(30) Konrat, R. Manuscript in preparation.

(31) Konrat, R.; Puchberger, M.; Kräutler, B.; Kratky, C.; Hoffman, E. To be submitted.

(32) Hurd, R. E.; John, B. K. *J. Magn. Reson.* **1991**, *91*, 648.

(33) Davis, A. L.; Keeler, J.; Laue, E. D.; Moskau, D. *J. Magn. Reson.* **1992**, *98*, 207.

(34) Bax, A.; Summers, M. F. *J. Am. Chem. Soc.* **1986**, *108*, 2093.

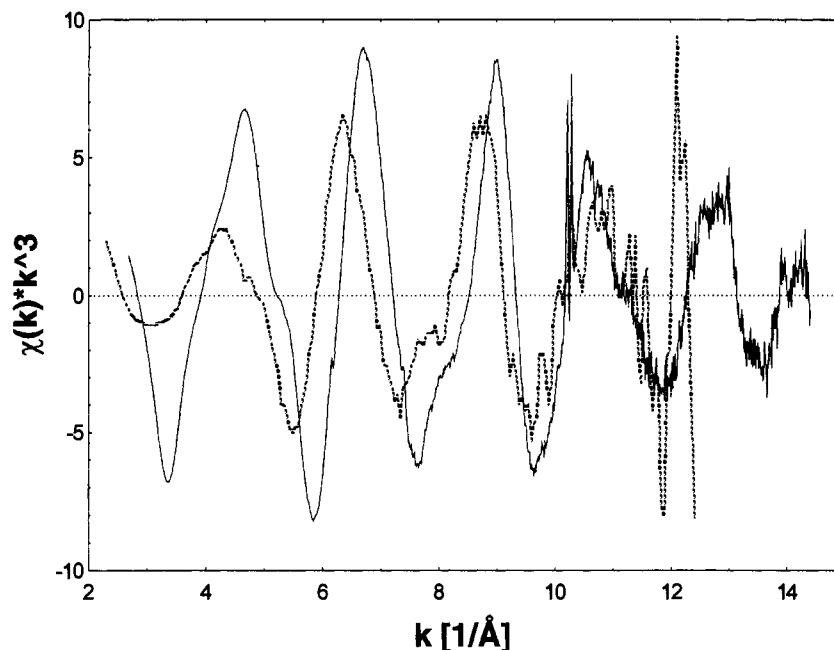


**Figure 8.** Comparison of the solution EXAFS spectrum of aquocobalamin perchlorate ( $1^+\text{ClO}_4^-$ ) (present work, solid line), with the "aquocobalamin" spectrum published in ref 5a (broken line).

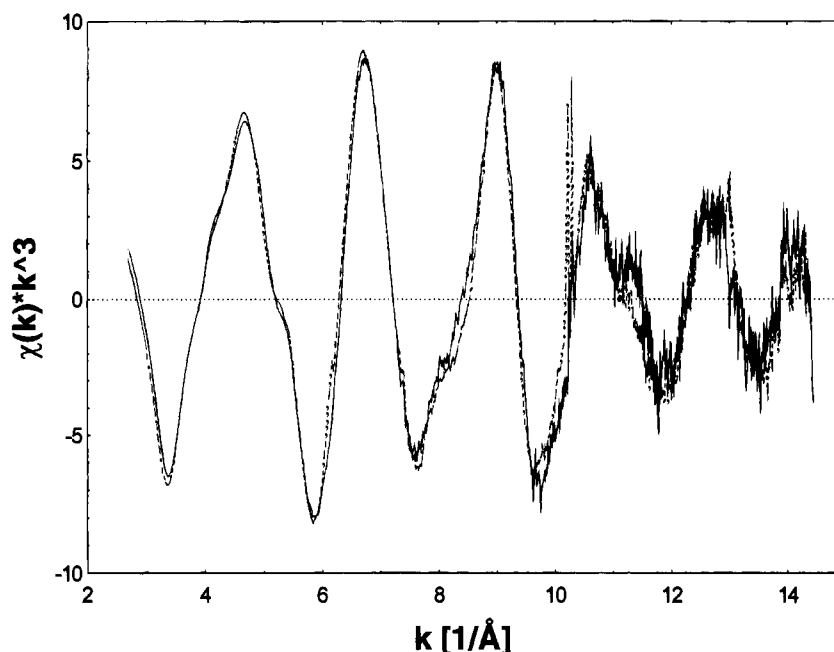


**Figure 9.** Superposition of the  $k^3$ -weighted EXAFS spectra of dissolved (broken line) and crystalline (solid line) aquocobalamin perchlorate ( $1^+\text{ClO}_4^-$ ).

analogy to literature assignments of the  $^{15}\text{N}$  resonances of other nitrogen heterocycles.<sup>35a</sup>

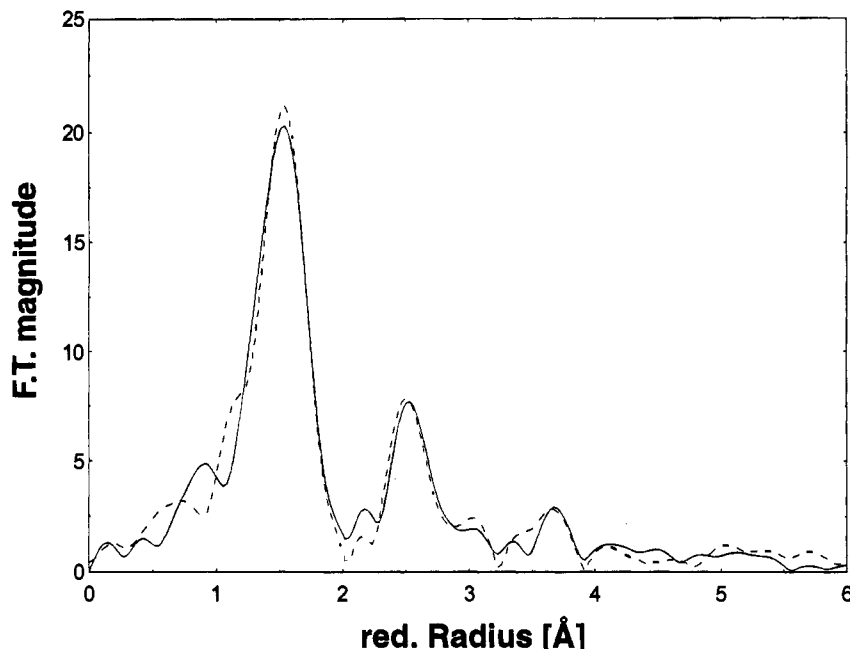
#### Evidence for Cobalt-Coordinated Water from NMR Data.

Figure S9 (supplementary material) shows a contour plot of a 200 ms "watergate" ROESY. The corresponding cross section parallel to the  $\omega_2$ -axis taken at the  $\omega_1$  frequency of the water resonance is shown in Figure 12. There are water NOEs found to protons located in the "upper" half (or  $\beta$ -side) of the molecule, such as protons at C26, C46, C54, and C19. These NOEs provide evidence for a water molecule located at the  $\beta$ -side, at

a roughly similar distance to these protons and with a resonance time longer than the reorientational correlation time of  $1^+$ .<sup>36</sup> This is compatible with a cobalt-coordinated water molecule. These NOEs could not be detected in the SS-NOESY experiment, where NOE between the water protons and the protons at B10, B11, C35, and C53 were still observed. This suggests that these latter water protons belong to less strongly bound "peripheral" water associated with the lower side ( $\alpha$ -side) of the molecule and having shorter residence times. Note that the positive cross peaks located at 5.50 and 3.88 ppm belong to exchange cross peaks with the bulk water signal: the proton resonating at 5.50 ppm could be assigned to the hydroxy proton

(35) (a) Brown, K. L.; Evans, D. R. *Inorg. Chem.* **1994**, *33*, 525. (b) Brown, K. L.; Evans, D. R.; Wu, G.-Z.; *Inorg. Chem.* **1993**, *32*, 4487. (c) Brown, K. L.; Brooks, H. B.; Gupta, B. D.; Victor, M.; Marques, H. M.; Scooby, D. C.; Groux, W. J.; Timkovich, R. *Inorg. Chem.* **1991**, *30*, 3430. (d) Brown, K. L.; Brooks, H. B.; Zou, X.; Victor, M.; Timkovich, R. *Inorg. Chem.* **1990**, *29*, 4841.

(36) At 500 MHz field strength and a temperature of 5 °C, the correlation time  $\tau_c$  of the reorientational motion of the aquocobalamin ion is slightly longer than critical ( $\tau_c \approx 360$  ps), leading to vanishing or small positive NOESY cross peaks.



**Figure 10.** Fourier transforms of the  $k^3$ -weighted EXAFS spectra for dissolved (broken line) and crystalline (solid line) aquocobalamin perchlorate ( $1^+\text{ClO}_4^-$ ).

**Table 1.**  $^{15}\text{N}$  and  $^1\text{H}$  (Amide protons) NMR Chemical Shifts and Signal Assignments for Aquocobalamin Chloride ( $1^+\text{Cl}^-$ )

assignment	$\delta$	
	$^{15}\text{N}^a$	$^1\text{H}$
N29	111.6	7.83/7.14
N34	104.5	7.63/6.91
N40	113.2	8.13/7.11
N45	102.3	6.46/6.42
N52	105.4	7.73/7.02
N59	113.5	8.19
N63	106.3	7.92/7.08
N21	143.9	
N22	191.3	
N23	183.6	
N24	150.8	
NB1	193.4	
NB3	255.5	

<sup>a</sup>  $^{15}\text{N}$  chemical shifts reported relative to  $\text{NH}_3(1)$ .

H(OR7) (TOCSY cross peak to R2), and the proton at 3.88 ppm was assigned to one of the methylene protons at R5. Thus the cross peak at 3.88 ppm is an exchange-relayed cross peak, typical of protons located in the vicinity of exchangeable protons.<sup>37</sup>

**Evidence for Hydrogen Bonding from NMR Data.** Our search for experimental evidence for hydrogen bonding in aqueous solution between the cobalt-coordinated water molecule and the carbonyl oxygen of the c-side chain was supported by several experiments: firstly, by distance constraints derived from the ROESY map (see Figure 11). There, NOEs were found between the H<sub>E</sub> amide proton and the protons H(C8), H<sub>a</sub>(C37), H<sub>b</sub>(C37), and H(C36), as well as between the H<sub>Z</sub> amide proton and H(C10) and the methyl group C46. The derived distance constraints indicate the amide NH<sub>2</sub> group to be pointing toward the "east" of the molecule and, accordingly, the carbonyl oxygen to be in close proximity to the cobalt-coordinated water molecule, allowing for H-bonding, as observed in the crystal structure.

Secondly, the exchange rates of the amide protons were measured as a function of pH. Exchange rates have proven to

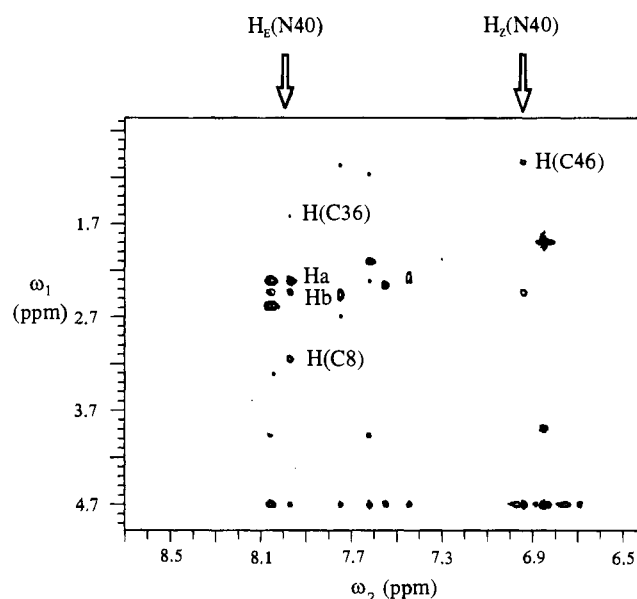


**Figure 11.** Spectral region of a "watergate" experiment (at 5 °C) containing the cross peaks between the amide protons and the high-field methylene protons. The cross peak positions of NOEs between the trans (H<sub>E</sub>) amide proton of the c-acetamide function (N40) and the side chain methylene protons are identified for the c-side chain.

be a very sensitive probe for solvent accessibility and hydrogen bond stability of amide protons in peptides and proteins.<sup>38</sup> Figure 13 shows the pH profile of the rates of proton exchange for the H<sub>E</sub> amide protons of the three acetamide functions. Note that the measured exchange rates comprise contributions stemming from intermolecular exchange to the solvent and intramolecular proton exchange or *E/Z* isomerization around the amide C–N bond. The three amide groups exhibit a characteristically different pH dependence (Figure 13). Typically, at low pH (acid-catalyzed) proton exchange of H<sub>E</sub>(N40) (c-acetamide) is slower than that of the H<sub>E</sub> protons of the other two amide groups, while the order of rates is reversed for the (base-catalyzed)

(37) Van de Ven, F. J. M.; Jansen, H. G. J. M.; Gräslund, A.; Hilbers, C. W. J. *Magn. Reson.* **1988**, *79*, 221.

(38) Englander, S. W.; Kallenbach, N. R. *Q. Rev. Biophys.* **1984**, *16*, 521.



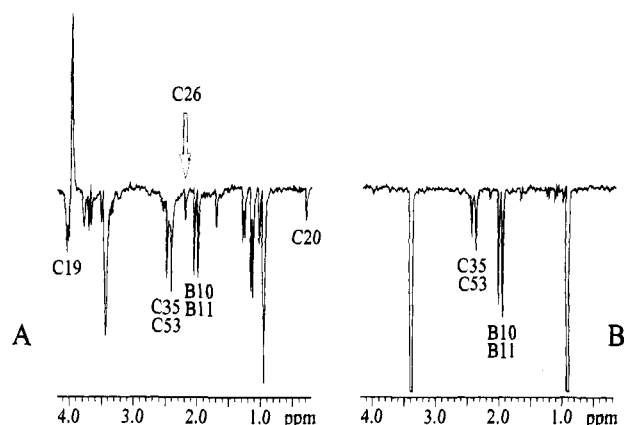


**Figure 12.** (A) Cross section parallel to the  $\omega_2$ -axis taken at the  $\omega_1$  frequency of the water resonance through the 200 ms "watergate" ROESY (see the deposited Figure S9 for the complete contour plot). (B) Corresponding cross section from a NOESY experiment.

process at a pH above  $\sim 3.5$ . Accordingly, displacement of the exchange profile by 0.3 unit to lower pH is observed for the  $H_E(N40)$ .

Figure 14 shows the intramolecular proton exchange peaks as off-diagonal elements between the  $H_Z$  and  $H_E$  amide protons of a-, b-, c-, e-, and g-amide functions at 5 and 26 °C. This was obtained from two "watergate" ROESY experiments. At 5 °C, negative cross peaks indicate insignificant contributions of amide exchange but essentially pure dipolar interaction. However, at 26 °C, the same situation applies only to the c-acetamide, indicating that the rotation around the C–N bond of the c-acetamide has a considerably higher barrier than that of the other primary amide groups. Note that exchange and dipolar contributions roughly cancel for the g-acetamide at 26 °C. Positive off-diagonal peaks are found for the a-, b-, and e-acetamide functions, indicating predominance of intramolecular proton exchange.

## Discussion

Homolysis of the cobalt–carbon bond of coenzyme  $B_{12}$  is understood to be the key step<sup>39</sup> initiating the sequence of reactions catalyzed by coenzyme  $B_{12}$  dependent enzymes, such as (methylmalonyl)-CoA mutase<sup>40</sup> and dioldehydrase.<sup>39</sup> The observed rates of the enzymatic reactions imply that homolysis of this bond occurs about  $10^{12}$  times faster<sup>41</sup> in the enzyme than in the water-solvated coenzyme.<sup>41</sup> The most generally accepted explanation for this large acceleration involves a conformational distortion of the bound coenzyme. Specifically, enzyme-induced "upward" deformation of the corrin ring was proposed as a means to facilitate Co–C bond homolysis via steric repulsion between the corrin ring and the desoxyadenosyl leaving group.<sup>15</sup> This "upward conformational deformation" theory was largely inspired by crystallographic observations on  $B_{12}$  model complexes, where the steric bulk of one or both axial ligands induces butterfly-type deformations of the equatorial ligands, together with changes in the axial bond lengths.<sup>11</sup> Similar effects are believed to occur in protein-bound coenzyme  $B_{12}$ . In line with

this argument is Halpern's proposition that the corrin ligand in coenzyme  $B_{12}$  characteristically exhibits a remarkable flexibility.<sup>42</sup>

Indeed, the main mode of structural variability of the corrin ring experimentally observed in crystal structures of  $B_{12}$  derivatives is an "upward" folding about a line running "east" to "west".<sup>43,23</sup> Recently, we analyzed the structure of Co- $\beta$ -cyanoimidazolylcobamide, a  $B_{12}$  derivative in which an imidazole replaces the dimethylbenzimidazole (DMB) base of vitamin  $B_{12}$ .<sup>7</sup> In this work, the upward folding deformation in these cyano cobalt(III) corrins was traced back to steric interactions between corrin ring and coordinated base, leading to a *stretch* of the Co– $N_{ax}$  bond, an increased *fold* of the corrin ring, and a *tilt* of the cobalt-coordinated nucleotide base.

Coordination chemistry and structural data on model complexes<sup>11</sup> strongly suggest that in a cobalamin with a very weak donor as  $\beta$ -ligand—such as water—the trans axial Co–N bond should be inherently short, i.e., the bond length should even be decreased compared to that in vitamin  $B_{12}$  (**2**).<sup>44</sup> This would necessarily lead to a further increase of the strain due to steric repulsion, and the question is of considerable interest as to which of the above parameters—axial Co–N bond length, base tilt, or corrin fold—would be most affected by the increased strain.

Solution–structure analysis of "aquocobalamin" by EXAFS led to the proposal of a very long axial Co–N distance of 2.14(3) Å,<sup>5a</sup> suggesting that the strain affects mainly the Co–N bond length. This would imply that the other parameter found to be sensitive to the steric repulsion between corrin ring and DMB base—the "upward folding"—would be "stiffer". Evidently this would then have implications for the upward conformational distortion model, since this hypothesis requires a flexible corrin ring. This dilemma, the general question of the distribution of strain in a complete corrin with a (inherently) very short axial Co–N bond, and the underlying question of the "mechanics" of the  $B_{12}$  system in view of its relevance to the mechanochemical distortion hypothesis formed the motivation behind the structure analysis of the aquocobalamin ion reported in this communication.

**Crystal Structure Analysis of Aquocobalamin Perchlorate ( $1^+ClO_4^-$ ).** In the aquocobalamin ion ( $1^+$ ), a very short axial Co–N bond of 1.925(0.002) Å was found crystallographically, the shortest Co–N bond observed so far in a "complete" corrinoid. This value is about 0.3 Å shorter than what is observed in organocobalamins, such as the biological cofactors methylcobalamin (**4**) ( $d(\text{Co}–N_{ax}) = 2.19$  Å)<sup>4h</sup> and coenzyme  $B_{12}$  (**3**) ( $d(\text{Co}–N_{ax}) = 2.24$  Å).<sup>4i</sup>

A short axial bond to the  $\alpha$ -ligand indeed is expected, on the basis of crystal structure data on  $B_{12}$  model complexes,<sup>11,44</sup> and is in line with the weak donor ability of water as the  $\beta$ -ligand. The "upward" movement of the coordinated DMB base toward the cobalt center increases steric repulsion between DMB base and corrin periphery. We have recently identified three major structural consequences of such interference,<sup>7</sup> namely, stretch of the axial Co–N bond, tilt of the DMB base, and (upward) fold of the corrin ring. Figure 7, which shows a superposition

(42) Geno, M. K.; Halpern, J. *J. Am. Chem. Soc.* **1987**, *109*, 1238.

(43) Pett, V. B.; Liebman, M. N.; Murray-Rust, P.; Prasad, K.; Glusker, J. P. *J. Am. Chem. Soc.* **1987**, *109*, 3207.

(44) (a) The difference in the electronic trans effect between water and cyanide axial ligands can be exemplified by a comparison of two cobaloxime crystal structures with a pyridine "lower" ligand and water<sup>44b</sup> and cyanide<sup>44c</sup> as respective upper ligands. Here, a decrease of the axial cobalt–nitrogen bond length from 1.938 to 1.915 Å is observed when exchanging  $CN^-$  by  $H_2O$  as upper ligand. (b) Attia, M. W.; Zangrando, E.; Randaccio, L.; Lopez, C. *Acta Crystallogr. C* **1987**, *43*, 1521. (c) Attia, W. M.; Zangrando, E.; Randaccio, L.; Antolini, L.; Lopez, C. *Acta Crystallogr. C* **1989**, *45*, 1500.

(39) Abeles, R. H. In *Vitamin B<sub>12</sub>, Proceedings of the Third European Conference*; Zagalak, B., Friedrich, W., Eds.; W de Gruyter: Berlin, 1979; p 373.

(40) Rétey, J. In *B<sub>12</sub>*; Dolphin, D., Ed.; Wiley: New York, 1982; Vol. 2, p 357.

(41) (a) Halpern, J. *Science* **1985**, *227*, 869. (b) Halpern, J.; Kim, S.-H.; Leung, T. W. *J. Am. Chem. Soc.* **1984**, *106*, 8317. (c) Finke, R. G.; Hay, B. P. *Inorg. Chem.* **1984**, *23*, 3043. (d) Hay, B. P.; Finke, R. G. *J. Am. Chem. Soc.* **1986**, *108*, 4820.

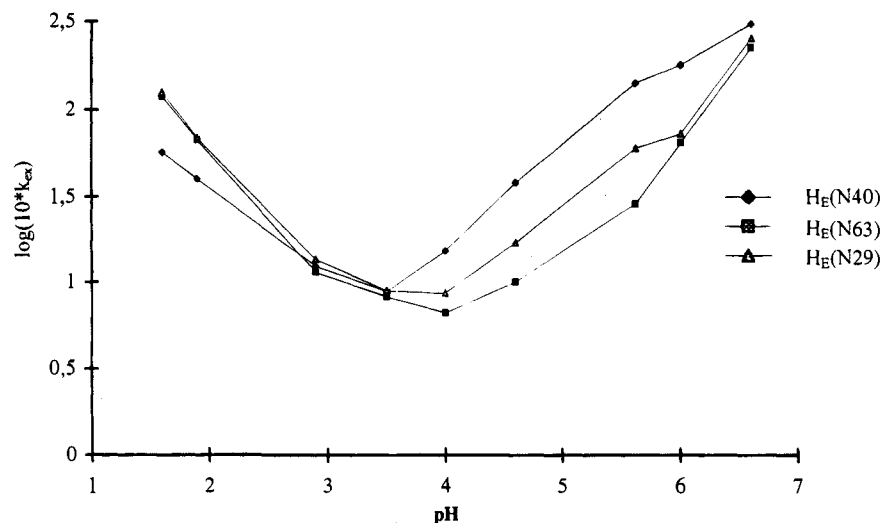


**Figure 13.** pH profile of the intermolecular proton exchange rates ( $s^{-1}$ ) of the trans ( $H_E$ ) amide protons of the three acetamide (a,  $H_b(N29)$ ; c,  $H_b(N40)$ ; g,  $H_b(N63)$ ) functions. The experimental data for each acetamide were fitted by a hyperbola, whose parameters (the asymptotes  $a(H^+)$  and  $a(OH^-)$  and the pH minimum  $pH_{min}$ ) have been calculated from a linear least-squares fit, yielding the following values: c-acetamide,  $a(H^+) = -0.44$ ,  $a(OH^-) = 0.50$ ,  $pH_{min} = 3.40$ ; a-acetamide,  $a(H^+) = -0.62$ ,  $a(OH^-) = 0.54$ ,  $pH_{min} = 3.70$ ; g-acetamide,  $a(H^+) = -0.64$ ,  $a(OH^-) = 0.57$ ,  $pH_{min} = 3.85$ .

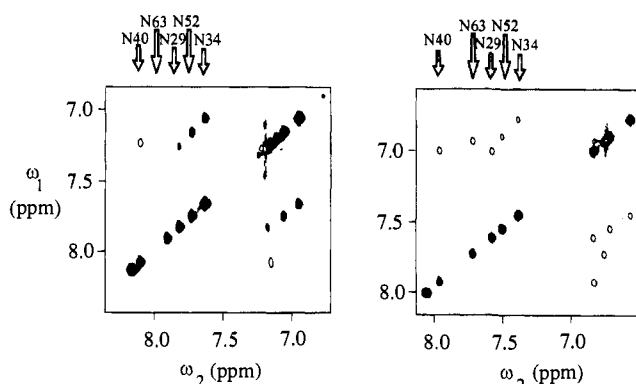


**Figure 14.** Low-field sections of two "watergate" ROESY experiments showing both dipolar and intramolecular exchange contributions. The two experiments were recorded at 5 °C (left) and 26 °C (right), respectively.

of parts of the crystal structures of  $1^+ClO_4^-$  and coenzyme B<sub>12</sub> (3), reveals that the base tilt is little affected by the 0.3 Å shortening of the Co–N<sub>ax</sub> bond. In fact a tilt<sup>25</sup> of the DMB base by about 5° appears to be an inherent property of cobalt complexes of dimethylbenzimidazole (as opposed to imidazole):<sup>7</sup> in all known cobalamin crystal structures<sup>4</sup> as well as in B<sub>12</sub> model complexes with DMB as axial ligand,<sup>45</sup> the "northern" Co–N<sub>ax</sub>–C angle was found to exceed the "southern" angle by about 10°. Also, the axial Co–N distance of 1.925 Å is quite similar to the corresponding distance of 1.927 Å observed in the crystal structure of a cobaloxime with water and pyridine occupying the two axial coordination sites,<sup>44b</sup> suggesting that steric repulsion between DMB and corrin ring does not lead to appreciable lengthening of the axial Co–N bond.

As Figure 7 suggests, the main conformational effect of the short axial Co–N bond is an increased upward flexing of the "northern" half of the corrin ring, resulting in an upward fold angle<sup>23</sup> of 18.71(0.07)° in the crystal structure of  $1^+ClO_4^-$ . It has been suggested earlier<sup>20</sup> that a steric repulsion between DMB base and corrin ring would mainly involve contacts between protons H(B2) and H(B4) and the "lower" side of the corrin

ring. Interestingly, upward movement of the DMB base toward the corrin ligand has different consequences for the two protons: the "northern" half of the corrin ring "yields" to the approach of the DMB base, increasing the upward folding while allowing the distance between H(B4) and the northern ring plane to approach a minimum value of ~2.3 Å. Proton H(B2) in contrast is moved with the DMB base "into" the southern half of the corrin ring, i.e., the distance between proton and ring plane decreases in parallel with the decreasing Co–N<sub>ax</sub> distance; a minimum value is not apparent from the data available (in crystals of  $1^+ClO_4^-$ , the distance between H(B2) and the "southern" ring plane amounts to 2.27 Å).

Thus, the long axial Co–N bond deduced for "aquocobalamin" from EXAFS data and ascribed to steric repulsion<sup>5a</sup> between corrin ring and DMB base is not observed in the solid state. Instead, the strain induced by the short Co–N<sub>ax</sub> bond as a result of the weak trans axial donor (H<sub>2</sub>O) is relieved by upward folding of the "northern" half of the corrin ring.

**Relevance for the Mechanochemical Distortion Hypothesis of Coenzyme B<sub>12</sub> and Other Organocobalamins.** It is tempting to relate the upward flexing of the corrin ring observed in the crystal structure of  $1^+ClO_4^-$  to the biological function of coenzyme B<sub>12</sub> (3), specifically with regard to the hypothesis of a conformationally induced activation of its Co–C bond toward homolysis. Clearly the cause for the (relatively) large upward deformation in  $1^+ClO_4^-$  crystals—a very short axial Co–N bond induced by a very weak donor as trans axial ligand—is unlikely to be of relevance in organocobalamins, where the very strongly donating β-ligands induce axial Co–N distances around 2.20 Å.<sup>20,4b,g,h,i,k</sup> Moreover, it is unclear whether enzyme-bound coenzyme B<sub>12</sub> is still in the base-on form.<sup>46</sup>

The crystal structure of  $1^+ClO_4^-$  is likely to contain the corrin ring with the largest upward deformation induced by weak trans electronic effects. In spite of this "extreme" example, the

(45) (a) Parker, W. O., Jr.; Zangrando, E.; Bresciani-Pahor, N.; Marzilli, P. A.; Randaccio, L.; Marcelli, L. G. *J. Am. Chem. Soc.* **1988**, *27*, 2170. (b) Charland, J.-P.; Zangrando, E.; Bresciani-Pahor, N.; Randaccio, L.; Marzilli, L. G. *Inorg. Chem.* **1993**, *32*, 4256.

(46) (a) A recently completed crystal structure analysis of the B<sub>12</sub> binding domain of methionine synthase<sup>46b</sup> shows the enzyme-bound methyl corrinoid cofactor in the base-off form, with the imidazole from a histidine residue occupying the α-axial metal coordination site. The chemical function of methylcobalamin as cofactor is different from that of adenosylcobalamin (heterolysis vs homolysis), and the evidence from sequence information for a similar binding of the B<sub>12</sub> cofactor in coenzyme B<sub>12</sub> dependent enzymes as observed in methionine synthase is still inconclusive. (b) Drennan, C. L.; Huang, S.; Drummond, J. T.; Matthews, R. G.; Ludwig, M. L. *Science* **1994**, *266*, 1669.

geometrical variation observed so far in cobalamins with respect to the upward folding is small, much smaller than what has been observed in model complexes<sup>11</sup> and hdroporphyrins.<sup>47</sup> Accordingly, the suggested biologically crucial flexibility of the corrin ring<sup>42</sup> appears to be rather restricted.

**Use of Synchrotron Radiation for B<sub>12</sub> Structure Analysis.** Crystal structure determinations of cobalamins<sup>48</sup> have notoriously suffered from poor accuracy due to the presence of a considerable number (10–30/B<sub>12</sub> molecule) of mostly disordered<sup>49</sup> solvent molecules.<sup>20,50</sup> However, use of synchrotron radiation in combination with an imaging plate detector yielded intensity data (22 867 unique and 20 942 significant ( $F_{\text{obs}} > 2\sigma F_{\text{obs}}$ ) reflections) permitting refinement of the crystal structure of  $1^+\text{ClO}_4^-$  with unprecedented accuracy. For the first time, the molecular geometry of a B<sub>12</sub> can be determined with the precision and reliability of real small-molecule crystallography ( $R = 0.050$  for all data). The low average standard deviation of bond lengths (0.003 Å for all C–C bonds) puts the crystal structure of  $1^+\text{ClO}_4^-$  into the class of the most accurate structures within the Cambridge Structural Data Base (average  $\sigma$  flag = 1)<sup>52</sup> and makes it comparable to a small-molecule structure with an  $R$ -value below 3%.<sup>53</sup>

**Position of the Hydrogen Atoms at the Cobalt-Coordinated Water Molecule.** The superior diffraction data permitted the direct observation of hydrogen atoms in difference electron maps. Figure 4 shows the difference density around the cobalt-coordinated water molecule, contouring the density originating from its two hydrogen atoms. Also shown are the positions of both atoms after restrained<sup>54</sup> least-squares refinement. As expected, the electron density maxima are displaced along the O–H vector toward the oxygen atom as a result of the deformation of the bonding electron density. While—in the absence of suitable restraints—this would decrease the apparent length of the O–H bonds, it should not affect the bond angles. Remarkably, the two hydrogen atoms, the water oxygen, and

the cobalt atom are nearly coplanar, with a sum of the three bond angles around O1x of 357°.

Since ligand-to-metal dative  $\pi$ -bonding<sup>55</sup> is unlikely for the Co(III) center, this observation is at first sight surprising, though not uncommon: a search in the Cambridge Structural Data Base<sup>52</sup> for high-resolution crystal structures of water molecules coordinated to cobalt(III) yielded 17 structure determinations with 20 symmetry independent fragments, of which eight had a bond angle sum around the water oxygen exceeding 350°. Apart from the electronic effects—which favor a tetrahedral oxygen atom with a bond angle sum of  $\approx 330^\circ$ —there are other effects which could favor a coplanar arrangement of metal, oxygen, and the two hydrogen atoms, e.g., steric and electrostatic<sup>55</sup> repulsion and possibly the formation of hydrogen bonds. Conclusive resolution of this question will have to await more unequivocal experimental evidence, expected from a neutron diffraction analysis of  $1^+\text{ClO}_4^-$ .

**Determination of the Solution Structure of Aquocobalamin Perchlorate ( $1^+\text{ClO}_4^-$ ) by EXAFS Spectroscopy.** The crystallographic data on  $1^+\text{ClO}_4^-$  are in disagreement with the cobalt coordination data obtained from an analysis of the EXAFS of a frozen solution of aquocobalamin ( $1^+$ ) in water/ethylene glycol.<sup>5a</sup> While the equatorial Co–N distances agree between the two determinations within the respective ESD's (EXAFS, Co–N(eq) =  $1.89 \pm 0.01$  Å; X-ray average of the four equatorial Co–N distances =  $1.89 \pm 0.01$  Å, with  $\sigma(\text{Co–N}) = 0.002$  Å for each of the four quantities, see Figure 3), the axial Co–N and Co–O distances are significantly different: EXAFS, Co–N(DMB) =  $2.14 \pm 0.03$  Å, Co–O(H<sub>2</sub>O) =  $1.90 \pm 0.02$  Å; X-ray, Co–N(DMB) =  $1.925(0.002)$  Å, Co–O(H<sub>2</sub>O) =  $1.952(0.002)$  Å. Of particular concern is the large difference (more than 0.2 Å) in the distance between cobalt and the nitrogen atom of the coordinating DMB base.

A similar disagreement between EXAFS and crystallographic results was noted for vitamin B<sub>12</sub> (**2**),<sup>7</sup> where the EXAFS data<sup>5a</sup> also suggest a larger (by  $\approx 0.14$  Å) axial Co–N distance. Originally, the long Co–N distances obtained from EXAFS were considered “unexpected” and suggested to arise from steric repulsions between the DMB ligand and the corrin ring.<sup>5a</sup>

Comparison of the crystallographic data on Co- $\beta$ -cyanoimidazolylcobamide and vitamin B<sub>12</sub> (**2**) conclusively showed<sup>7</sup> that such a repulsion between the DMB ligand and the corrin ring indeed exists and leads to distortions of the Co–N–C bond angles, an increase in the corrin fold angle, and a lengthening of the Co–N(ax) bond. In the solid state, this lengthening amounted to  $\approx 0.04$  Å for cyanocobalamin. The crystallographic data thus show that there is indeed strain which tends to lengthen the Co–N bond and/or fold the corrin ring, but the Co–N bond appears to be “stiffer”, relegating most of the deformation to the corrin ring folding.

In summary, the EXAFS results disagree with the available other structural data, including indirect evidence from a recent NMR study on aquocobalamin acetate ( $1^+\text{Ac}^-$ ).<sup>9</sup> Disagreement between crystallographic and EXAFS results was also noted for cob(II)alamin B<sub>12</sub>, where EXAFS<sup>5b</sup> obtained an axial Co–N distance shorter by 0.15 Å than the crystal structure analysis.<sup>4j</sup>

(55) Cotton, F. A.; Fair, C. K.; Lewis, G. E.; Mott, G. N.; Ross, F. K.; Schultz, A. J.; Williams, J. M. *J. Am. Chem. Soc.* **1984**, *106*, 5319.

(56) (a) Attia, M. W.; Zangrando, E.; Randaccio, L.; Lopez, C. *Acta Crystallogr. C* **1987**, *43*, 1521. (b) Bernauer, K.; Stoekli-Evans, H.; Hugli-Cleary, D.; Hilgers, H. J.; Abd-el-Khalek, H.; Porret, J.; Sauvain, J.-J. *Helv. Chim. Acta* **1992**, *75*, 2327. (c) Bresciani-Pahor, N.; Randaccio, L.; Toscano, P. J.; Marzilli, L. G. *J. Chem. Soc., Dalton Trans.* **1982**, 567. (d) Brown, S. J.; Hudson, S. E.; Mascharak, P. K.; Olmstead, M. M. *J. Am. Chem. Soc.* **1989**, *111*, 6446. (e) Kanamori, K.; Broderick, W. E.; Jordan, R. F.; Willett, R. D.; Legg, J. I. *J. Am. Chem. Soc.* **1986**, *108*, 7122. (f) Mutikainen, I. *Finn. Chem. Lett.* **1985**, 193. (g) Rawji, G. H.; Lynch, V. M. *Acta Crystallogr. C* **1992**, *48*, 1667.

(47) Kratky, C.; Waditschatka, R.; Angst, C.; Johansen, J. E.; Plaquevent, J. C.; Schreiber, J.; Eschenmoser, A. *Helv. Chim. Acta* **1985**, *68*, 1312.

(48) X-ray structure determinations of the following “complete corrinoids” (i.e., cobamides with an intramolecularly coordinating nucleotide base) have been reported so far (multiple structure determinations on the same compound, i.e., for **2** and **3**, have only been listed once, with the most recent analysis): vitamin B<sub>12</sub>-5'-phosphate,<sup>4c</sup>  $R = 0.162$ ; 13-epi-cyanocobalamin,<sup>4d</sup>  $R = 0.159$ ; Co $\beta$ -cyano(2-(methyladeninyl)cobamide),<sup>4e</sup>  $R = 0.166$ ; cyanocobalaminmonocarboxylic acid,<sup>4f</sup>  $R = 0.140$ ; (S)-(2,3-dihydroxypropyl)cobalamin,<sup>4g</sup>  $R = 0.151$ ; methylcobalamin,<sup>4h</sup>  $R = 0.146$ ; cyanocobalamin (**2**),<sup>4a,7</sup>  $R = 0.086$ ; superoxocobalamin,<sup>4i</sup>  $R = 0.095$ ; cob(II)alamin B<sub>12</sub> (**6**),<sup>4j</sup>  $R = 0.102$ ; adeninylpropylcobalamin,<sup>4k</sup>  $R = 0.100$ ; 5'-deoxyadenosylcobalamin (**3**),<sup>4b,j</sup>  $R = 0.088$ ; (R)-2,3-dihydropropylcobalamin,<sup>4g</sup>  $R = 0.085$ ; Co $\beta$ -cyanoimidazolylcobamide,<sup>7</sup>  $R = 0.102$ ; cyano-8-epicobalamin,<sup>4m</sup>  $R = 0.052$ .

(49) A notable exception to the presence of a large number of partially disordered solvent molecules is the crystal structure of adenylpropylcobalamin,<sup>4k</sup> which contained 10 fully ordered water molecules per B<sub>12</sub>. Even in this case, the structure could not be refined beyond  $R = 0.1$ .

(50) Savage and Finney<sup>51</sup> have demonstrated that much can be gained from a careful analysis of the distribution of solvent sites in the crystal structure<sup>4i</sup> of the B<sub>12</sub> coenzyme (**3**).

(51) (a) Savage, H. F. *J. Biophys. J.* **1986**, *50*, 947. (b) Savage, H. F. *J. Ibid.* **1986**, *50*, 967. (c) Vovelle, F.; Goodfellow, J. M.; Savage, H. F. J.; Barnes, P.; Finney, J. L. *Eur. Biophys. J.* **1985**, *11*, 225. (d) Savage, H.; Wlodawer, A. *Methods Enzymol.* **1986**, *127*, 162. (e) Savage, H. F. J.; Finney, J. L. *Nature* **1986**, *322*, 717. (g) Finney, J. L.; Savage, H. F. *J. Mol. Struct.* **1988**, *177*, 23. (h) Bouquiere, J. P.; Finney, J. L.; Lehmann, M. S.; Lindley, P. F.; Savage, H. F. *J. Acta Crystallogr. B* **1993**, *49*, 79. (52) Allen, F. H.; Kennard, O.; Taylor, R. *Acc. Chem. Res.* **1983**, *16*, 146.

(53) (a) Allen, F. H. In *Accurate Molecular Structures*; Domenicano, A., Hargittai, I., Eds.; International Union of Crystallography, Oxford Univ. Press: New York, 1992; p 455. (b) Allen, F. H.; Doyle, M. J. *Acta Crystallogr. A* **1987**, *43*, C291.

(54) The following distance restraints were applied to the two hydrogen atoms at the metal-coordinated water molecule:  $d(\text{O–H}) = 0.95$  Å;  $d(\text{H}\cdots\text{H}) = 1.56$  Å.

It is unlikely that the discrepancies result from inaccuracies or errors in the X-ray data, since several crystal structures would then have to be grossly in error, including the present one of  $1^+\text{ClO}_4^-$ . If EXAFS and X-ray results are both reliable, we are left with the possibility of genuine structural differences between solution<sup>57</sup> and crystalline state. Surprising as a change in the Co–N bond length by 0.2 Å upon dissolving crystals containing  $1^+$  would be, the observation of different structural responses to steric repulsion between corrin ring and DMB base (stretch of the Co–N bond and fold<sup>23</sup> of the corrin ring) opens, at least in principle, the possibility that these counteracting deformations could be so well balanced that a lengthening of the axial Co–N bond *together* with a decrease in corrin fold and/or base tilt might become affordable by solvation energies.

To test for this possibility, we decided to repeat and extend some of the EXAFS measurements of Sagi and Chance.<sup>5a,b</sup> Figure 8 shows the EXAFS of a solution of aquocobalamin perchlorate ( $1^+\text{ClO}_4^-$ ) (solid line) with the “aquocobalamin” solution spectrum from ref 5a superimposed (dashed line). Figure S7 (supplementary material) gives the EXAFS of an *authentic* sample of the aquocobalamin perchlorate crystals used for the X-ray crystal structure determination. A superposition of the two spectra (solid and dissolved  $1^+\text{ClO}_4^-$ ) is shown in Figure 9. Compared to the spectra from ref 5a, our data extend to higher resolution and they show a lower noise level. It also appears that the two solution spectra of Figure 8 have a different shape.<sup>58</sup>

Irrespective of any structural interpretation of the spectra shown in Figure 9, it is evident that they superimpose very well.<sup>59</sup> If the EXAFS spectra are at all sensitive to changes in the coordination around cobalt, we can safely conclude that they contain no indication of major structural differences between the “solid state” and the “solution” of aquocobalamin perchlorate ( $1^+\text{ClO}_4^-$ ). Similar, but due to larger noise on the EXAFS solution spectra, less compelling results were obtained for vitamin B<sub>12</sub> and B<sub>12r</sub>.<sup>61</sup>

**Spectra Simulations and Curve Fitting.**<sup>60</sup> The near identity of solution and solid-state EXAFS spectra of  $1\text{ClO}_4^-$  (Figure 9) could also be the result of an insensitivity of the spectra to existing structural differences. We have carried out EXAFS simulations with the program EXCURV92,<sup>62</sup> using the coordination data from the crystal structure of  $1^+\text{ClO}_4^-$  and ref 5a. Irrespective of the approximation used, we have consistently observed differences between the simulated spectra for the two coordination geometries which were much larger than the

(57) It is frequently noted that EXAFS spectroscopy investigates the structure in “solution”, as opposed to crystallography, which investigates the “solid state”. This is often meant to imply that the “solution” is closer to the biologically relevant state, which is a questionable claim in the present situation: EXAFS experiments were carried out from solutions of aquocobalamin in a 1:2 mixture of ethylene glycol and water, flash-cooled to 100 K, whereas the crystallographic experiments were performed at ambient conditions with crystals grown from pure water, containing the B<sub>12</sub> species in a highly solvated form.

(58) Much of the differences in the EXAFS spectra of Figure 8, i.e., between solution spectra of aquocobalamin obtained by us (solid line) and by Sagi and Chance,<sup>5a</sup> is likely to be due to a different choice of  $E_0$ . We used a value of  $E_0 = 7717$  eV; no value for  $E_0$  is given in ref 5a.

(59) This is particularly true for the phases (i.e., the zero-crossings of the spectra), which should be different if there were a difference in the axial Co–N distance between the two spectra. The small differences observed for the amplitudes are barely above the noise level and may reflect minor changes in higher shells.

(60) We thank one of the referees for suggesting the first-shell curve-fitting calculations.

(61) Gruber, K.; Nolting, H.-F.; Kräutler, B.; Kratky, C. Manuscript in preparation.

(62) (a) Gurman, S. J.; Binsted, N.; Ross, I. *J. Phys. C* **1984**, *17*, 143. (b) Binsted, N.; Campbell, J. W.; Gurman, S. J.; Stephenson, P. C. *SERC Daresbury Laboratory EXCURV92 Program*; Daresbury: U.K., 1991.

**Table 2.** EXAFS Curve-Fitting Parameters and Results for Aquocobalamin Perchlorate ( $1^+\text{ClO}_4^-$ ) in the Crystalline State and in Solution, Assuming a Model with Only Co–N Interaction<sup>a</sup>

sample	BTR (Å)	$\Delta E_0$ (eV)	$N$	$r$ (Å)	$2\sigma^2$ ( $10^{-3}$ Å <sup>2</sup> )
crystalline	1.0–2.05	$18.3 \pm 0.6$	$6.0 \pm 0.3$	$1.90 \pm 0.01$	$6.4 \pm 0.3$
solution	0.9–2.0	$19.0 \pm 0.6$	$6.1 \pm 0.3$	$1.90 \pm 0.01$	$6.2 \pm 0.3$

<sup>a</sup> Parameters: BTR, back-transformation range (reduced radius);  $\Delta E_0$ , individual threshold energy offset (relative to  $E_0 = 7717$  eV);  $N$ , coordination number;  $r$ , average distance;  $2\sigma^2$ , Debye–Waller factor.

differences between the experimental spectra of dissolved and crystalline  $1^+\text{ClO}_4^-$  (Figure 9).<sup>63</sup> Thus, the presence of the proposed long (2.14 Å) Co–N distance should in any case be detectable by EXAFS spectroscopy.

Another question concerns the *consistency* of crystallographic and EXAFS results. With the resolution of the available EXAFS data (around 0.09 Å), it is clearly impossible to resolve individual distances within the octahedral Co coordination for the crystalline sample, where these distances are known from crystallography to differ by a maximum of 0.07 Å. The structural interpretation of the EXAFS data was thus restricted to an analysis of the first coordination shell, assuming a cobalt center surrounded by about six nitrogen atoms and aiming at a determination of an *average* Co–N distance. To that end, we separated the first-shell contributions via Fourier filtering (see Figure 10) of the  $k^3$ -weighted EXAFS and analyzed these data with a one-shell curve-fitting analysis varying  $E_0$ , the coordination number  $N$ , the (average) distance  $r$ , and the Debye–Waller factor  $2\sigma^2$ . The results are summarized in Table 2, yielding (within experimental uncertainty) a coordination number of 6 and an average Co–N distance of 1.90 Å for both samples. The errors in the derived parameters (see Table 2) are conservative estimates based upon a systematic analysis of model compounds.<sup>64</sup> Such error estimates are known to be larger and more realistic than the standard deviations derived from the least-squares variance–covariance matrix, particularly when the first-shell coordination distances are not uniform. Within the respective uncertainties, the structural parameters for the first Co coordination sphere are therefore consistent between the results from EXAFS and X-ray crystallography, and the EXAFS parameters of the solution sample are the same as those of the crystalline sample.

Thus, the long Co–N<sub>ax</sub> distance deduced from EXAFS spectra for aquocobalamin ( $1^+$ ) by Sagi and Chance<sup>5a</sup> could not be confirmed. While we do not wish to comment on possible causes for the disagreement,<sup>8</sup> we are pleased to recognize the available crystallographic evidence as representative of the structure of B<sub>12</sub> molecules in the solid state *and* in solution.

**Investigation of the Solution Structure of Aquocobalamin Chloride by NMR Spectroscopy.** NMR experiments performed in aqueous solution (H<sub>2</sub>O) are hampered by the intense water signal, which causes severe “dynamic range” problems. Thus, NMR experiments have been performed in deuterated solvents, e.g., D<sub>2</sub>O. Unfortunately, under these conditions amide protons exchange for solvent deuterium and become unobservable. Alternatively, by changing to an aprotic solvent, solvent-induced effects (conformational changes and/or chemical shift displacements) become important and make the extension of NMR data to physiological conditions unreliable. Therefore, NMR measurements in aqueous solution are desirable. A

(63) Gruber, K. Ph.D. Thesis, University of Graz, 1994.

(64) Eggers-Borkenstein, P.; Priggemeyer, S.; Krebs, B.; Henkel, G.; Simonis, U.; Pettifer, R. F.; Nolting, H. F.; Hermes, C. *Eur. J. Biochem.* **1989**, *186*, 667.

number of solvent suppression schemes for pulsed FT NMR in H<sub>2</sub>O solution have been proposed.<sup>65,66</sup>

Here we report the first comprehensive NMR analysis of a B<sub>12</sub> derivative in H<sub>2</sub>O. For this purpose, we have introduced into the field of B<sub>12</sub> NMR state-of-the-art water suppression techniques (e.g., symmetrically shifted shaped pulses<sup>67</sup> and watergate techniques<sup>68</sup> in combination with pulsed field gradients) that allowed us to assign all the exchangeable amide protons and their adjacent nitrogens.

**Signal Assignments.** Our assignment essentially confirmed data given by Calafat and Marzilli for the nonexchangeable protons of 1<sup>+</sup> and measured in D<sub>2</sub>O.<sup>9</sup> However, we could also detect the signal of the hydroxyl proton H(OR7) of the ribose unit at 5.50 ppm. We believe this to be the first indication of a water bridge in solution, linking the polar phosphate group and the hydroxyl group at R2, which causes a significant decrease in the intermolecular exchange to the solvent of this hydroxyl proton.<sup>31</sup> A highly conserved water site is found in crystal structures of 1<sup>+</sup>ClO<sub>4</sub><sup>-</sup> and other cobalamins.<sup>69</sup> The hydroxyl proton H(OR8) is still unobservable due to very efficient intermolecular exchange. This is indirectly seen in the ROESY experiment, where the R5 methylene protons exhibit very intense exchange-relayed cross peaks to the water, mediated via the H(OR8) hydroxyl proton (see Figures 12 and S9 of the supplementary material).

In combination with the X-ray data, the apparently "erratic" behavior<sup>9</sup> of the benzimidazole protons H(B2) and H(B4) is understandable. Both of these protons are localized at a distance from the respective half of the corrin ligand which is extremely short for a nonbonded interaction, i.e., at 2.27 Å (H(B2)) and 2.33 Å (H(B4)). H(B2) and H(B4) experience an upfield shift of 1.91 and 1.02 ppm, respectively, compared to the chemical shift of the corresponding signals of α-ribazole protons. For comparison, in vitamin B<sub>12</sub>, the corresponding chemical shift difference amounts to 1.31 and 0.95 ppm only, in agreement with the associated distances between the corrin ligand and H(B2) as well as H(B4) of 2.43 and 2.30 Å. As analyzed earlier by Brown and Hakimi<sup>70</sup> and Calafat and Marzilli,<sup>9</sup> shielding results from nonbonded axial contacts with the cobalt-coordinated plane. Unusual high-field shifts of protons of the nucleotide base accordingly may be an indication of short contacts with the corrin ring.

Unambiguous assignment of the amide protons was readily achieved due to specific NOEs between the amide protons and side chain methylene protons. These dipolar interactions also helped to discriminate between the two nitrogen-bonded amide protons, since only H<sub>E</sub> (the amide proton which is trans to the carbonyl oxygen) can be close in space to the α-methylene protons of the carboxamide functions. Its signal is consistently shifted to lower field, compared to the signal of the cis amide proton (H<sub>Z</sub>). Apparently, this consistent shift difference of signals of the H<sub>E</sub> and H<sub>Z</sub> protons of primary amide functions found here in aqueous solution also prevails in the spectra of base-on cobalamins in DMSO.<sup>71,72</sup> Compared to an NMR study

of 1<sup>+</sup> in DMSO,<sup>71,73</sup> there is a significant downfield shift of the proton resonances of the c- and f-acetamide functions, which provides good evidence for strongly different solvation effects (hydrogen bonding) on 1<sup>+</sup> upon changing the solvent. Furthermore, a specific high-field shift of the amide protons H(N45) and also their near isochronicity (implying a high-field shift of H<sub>E</sub>(N45)) are both fully compatible with the d-side chain conformation indicated in the crystal structure and can be explained by a specific shielding effect of the nearby coordinated DMB base.

Once all the amide protons had all their signals assigned, the amide nitrogen resonances could be analyzed in a straightforward manner by using connectivity data provided by a 2D <sup>1</sup>H-<sup>15</sup>N PFG-HSQC experiment. The resonances appear in the order (from high field to low field) N45, N34, N52, N63, N29, N40, and N59. As for amide protons, compared to <sup>15</sup>N amide signal assignments reported for a solution of 1<sup>+</sup> in DMSO,<sup>71,73</sup> there are significant downfield shifts of the c- and f-amide nitrogen signals. By use of the <sup>1</sup>H-<sup>15</sup>N PFG-HMBC experiment, optimized for a coupling of about 5 Hz, we could also (indirectly) observe and assign the corrin nitrogens N21, N22, N23, and N24, as well as the axial nucleotide nitrogens NB1 and NB3. Accordingly, there is a remarkable *relative* difference in the <sup>15</sup>N chemical shifts between NB1 and NB3 in aqueous solution compared to the situation in DMSO.<sup>71,73</sup> This is of interest as <sup>15</sup>N NMR chemical shifts of the axial nucleotide and the corrin ring have been used to estimate inductive, resonance, and steric substituent effects in alkylcobalamins,<sup>35</sup> as well as to demonstrate the implications of the correct resonance assignment on biosynthetic pathways.<sup>74</sup> Of course, nitrogen chemical shifts are sensitive to solvent effects (polarity, hydrogen bonding<sup>75</sup>).

**Evidence for Cobalt-Coordinated Water.** The watergate ROESY experiment allowed for the detection of exchangeable protons because it avoids water presaturation. This experiment not only enabled the assignment of these exchangeable protons but also provided information about the solution structure of the aquocobalamin ion (1<sup>+</sup>). Conformational information was obtained from ROESY data by comparing the observed intensities with internuclear distances observed in the crystal structure. Table 3 gives a list of structurally relevant NOE cross peak areas and associated interproton distances derived from the crystal structures of 1<sup>+</sup>ClO<sub>4</sub><sup>-</sup> and Co<sub>β</sub>-aquo-Co<sub>α</sub>-cyanocobyrinic acid.<sup>26</sup> The NOE-derived qualitative distance information is not compatible with the conformation of the c-side chain, as determined in the crystal structure analysis of 1<sup>+</sup>ClO<sub>4</sub><sup>-</sup> (see Figure 15, top). The data rather fit an average conformation matching that found in the crystal structure of aquocyanocobyrinic acid (see Figure 15, bottom). Accordingly, the H-bonding c-acetamide chain of 1<sup>+</sup> exhibits a conformation, in which the side chain points "south" with a synclinal arrangement of the bonds C8-C7 and C37-C38 (in aquocyanocobyrinic acid,<sup>26</sup> and torsion angle τ(C8-C7-C37-C38) = -52°); in crystalline 1<sup>+</sup>ClO<sub>4</sub><sup>-</sup>, these bonds are nearly antiperiplanar (τ = -157.8°). Thus, in aqueous solution, for the c-acetamide group of 1<sup>+</sup>, hydrogen bonding to the cobalt-coordinating water is indicated to arise from a time-averaged conformation which resembles that in the crystalline cobyrate (Figure 15, bottom) and not that of crystalline aquocobalamin 1<sup>+</sup>ClO<sub>4</sub><sup>-</sup> (Figure 15, top).

In addition, distance constraints for the amide group of the e-side chain also impose a different (average) orientation of this

(65) Hore, P. J. *Methods Enzymol.* **1989**, 176, 64.

(66) Gueron, M.; Plateau, P.; Decors, M. *Prog. NMR Spectrosc.* **1991**, 23, 135.

(67) Smallcombe, S. H. *J. Am. Chem. Soc.* **1993**, 115, 4776.

(68) Piotto, M.; Sautek, V.; Sklenar, V. *J. Biomol. NMR* **1992**, 2, 661.

(69) Hodgkin, D. C. *Angew. Chem.* **1964**, 77, 954.

(70) Brown, K. L.; Hakimi, J. M. *J. Am. Chem. Soc.* **1986**, 108, 496.

(71) Brown, K. L.; Evans, D. R. *Inorg. Chem.* **1993**, 32, 2544.

(72) In ref 71 the downfield proton resonance of the side chain primary amides were assumed to represent the E amide proton and the upfield resonance the Z amide proton, in agreement with assignments made earlier for various primary amides. See ref 71 and references therein.

(73) In the experiments reported in ref 71 it is unclear whether the cobalamin dissolved in DMSO carries H<sub>2</sub>O or DMSO as upper ligand.

(74) Hollenstein, R.; Stupperich, E. *Helv. Chim. Acta* **1993**, 76, 1258.

(75) Levy, G. C.; Lichter, R. L. *Nitrogen-15 Nuclear Magnetic Resonance Spectroscopy*; Wiley-Interscience: New York, 1979; Chapter 6.

**Table 3.** Comparison between Interproton Distances Obtained from Crystal Structure Data and ROESY Intensities<sup>a</sup>

H-H pair	H-H distances (Å)		ROESY
	1 <sup>+</sup> ClO <sub>4</sub> <sup>-</sup>	H <sub>2</sub> O-CN-cobyr	
H <sub>E</sub> (N40)-H <sub>a</sub> (C37)	2.196 <sup>b</sup>	2.04 <sup>c</sup>	100
H <sub>E</sub> (N40)-H <sub>b</sub> (C37)	3.251 <sup>b</sup>	3.27 <sup>c</sup>	35
H <sub>Z</sub> (N40)-H <sub>a</sub> (C37)	3.279	3.20	10
H <sub>Z</sub> (N40)-H <sub>b</sub> (C37)	3.797	3.83	
H(C8)-H <sub>a</sub> (C37)	2.494	2.16	100
H(C8)-H <sub>b</sub> (C37)	2.332	3.43	50
H(C36)-H <sub>a</sub> (C37)	2.515	2.48	strong NOE
H(C36)-H <sub>b</sub> (C37)	3.519	2.55	
H <sub>E</sub> (N40)-H(C8)	4.630	2.46	63
H <sub>Z</sub> (N40)-H(C8)	5.606	3.39	
H <sub>E</sub> (N40)-H(C36)	2.790	4.37	
H <sub>Z</sub> (N40)-H(C36)	3.622	5.57	
H <sub>Z</sub> (N40)-H(C46)	7.122	3.96	31
H <sub>E</sub> (N40)-H(C10)	6.525	3.86	
H <sub>Z</sub> (N40)-H(C10)	7.177	3.94	10
H(C54)-H <sub>2</sub> O	3.280	4.11	74
H(C46)-H <sub>2</sub> O	3.207	3.19	80
H(C26)-H <sub>2</sub> O	3.118	2.77	31
H(C26)-H(C19)	2.090	2.03	210
H(C26)-H <sub>b</sub> (C60)	3.578	3.34	27
H(C26)-H <sub>a</sub> (C60)	2.050	2.43	36
H(C26)-H(C25)	2.541	2.17	74
H <sub>E</sub> (N52)-H(R5)	3.415		
H <sub>Z</sub> (N52)-H(R5)	4.535		12
H <sub>E</sub> (N52)-H(C49)	2.322	2.30	42
H <sub>Z</sub> (N52)-H(C49)	3.349	3.44	

<sup>a</sup> For the crystallographically disordered methylene protons at R5 as well as for the methyl protons (C46, C54), a conformation with minimum interproton distance is given. <sup>b</sup> Data from the present work; H<sub>a</sub> = H<sub>si</sub>; H<sub>b</sub> = H<sub>re</sub> (assignment from comparison of X-ray distances and ROE intensities). <sup>c</sup> Data for aquocyanocobyrinic acid from ref 26; H<sub>a</sub> = H<sub>si</sub>; H<sub>b</sub> = H<sub>re</sub> (assignment from comparison of X-ray distances and ROE intensities).

amide group than that observed in the crystal structure of 1<sup>+</sup>ClO<sub>4</sub><sup>-</sup>. In particular, only the H<sub>Z</sub> amide proton oriented cis to the carbonyl oxygen, but not the H<sub>E</sub> amide proton of the e-amide group, shows weak NOEs to one of the (crystallographically disordered) protons at R5. This is not consistent with the crystal structure of 1<sup>+</sup>ClO<sub>4</sub><sup>-</sup>, where H<sub>E</sub>(N52) would be closer in space to R5 than H<sub>Z</sub>(N52) (see Table 3). The unambiguous assignment as H<sub>E</sub> or H<sub>Z</sub> was possible due to significant differences in intensities of NOEs to the e-side chain methylene protons at C49. This suggests that the time-averaged structure of 1<sup>+</sup> in solution differs from that in the solid state with respect to the conformation of the e-side chain.

The presence of a cobalt-coordinated water molecule was deduced by means of direct NOEs between protons of the β-side and water protons. Exchange of protons between cobalt-bound water and bulk water is fast on the chemical shift time scale, resulting in the observation of only one water signal in the spectrum. The presence of an NOE at the water chemical shift is thus indicative of a dipolar interaction between water protons either located in the "hydration sphere" or bound to the cobalt atom and protons of aquocobalamin. In order to discriminate between different water molecules with respect to the lifetimes of their bound state, we also conducted a SS-NOESY<sup>67</sup> experiment.<sup>36</sup> The fact that NOEs between water and the protons H(C19), H(C54), H(C26), and H(C46) are present in the ROESY experiment but absent in the NOESY experiment indicates a specific water molecule at the β-coordination site of the corrin-bound cobalt center with a residence time of the order of at least nanoseconds. In addition, there are several other cross peaks in the ROESY and NOESY spectra which cannot be explained by interactions through space with the cobalt-coordinated water. In particular, this is true for NOE

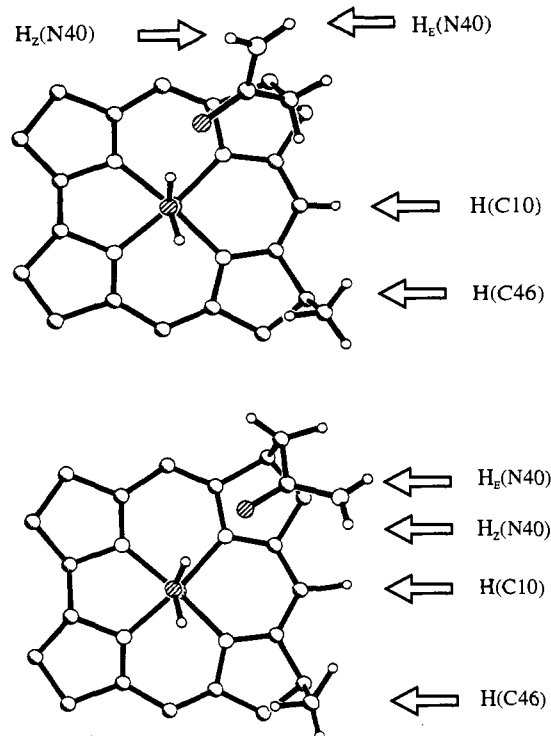


**Figure 15.** Axial projections of structure segments of aquocobalamin (1<sup>+</sup>; top) and of aquocyanocobyrinic acid (bottom). The figure exhibits atomic positions of corrin ring carbons and nitrogens, cobalt, cobalt-coordinated H<sub>2</sub>O, c-acetamide function, H(C10), and methyl group C46 of the two B<sub>12</sub> derivatives according to X-ray structure analyses. Structural data for 1<sup>+</sup> are from the present investigation and for aquocyanocobyrinic acid from ref 26.

cross peaks between the water signal and, for example, the signal of methyl groups on the lower half (α-side) Pr3, C20, C25, C47, B10, and B11, as well as the methyl groups C35 and C53. These NOEs provide evidence for associated water molecules located between the propionamide side chains and around the polar phosphate group, respectively. More details concerning the NMR analysis of the hydration behavior of vitamin B<sub>12</sub> derivatives in aqueous solution will be given elsewhere.<sup>31</sup>

**Evidence for a Specific Hydrogen-Bonding Interaction of the c-Acetamide Function.** It has been shown that acid-catalyzed exchange of amide protons with solvent water (intermolecular exchange) is diminished upon hydrogen bonding of the oxygen, thus resulting in a displacement of the exchange profile by 0.5–1.0 unit to lower pH.<sup>76</sup> Examination of the pH versus rate profile for hydrogen exchange of amide protons with bulk water indicated the c-acetamide group to exchange its protons slower at a pH smaller than ~3.5 but faster at a pH above ~3.5 than the other two acetamide functions. Thus, an increased resistance against acid-catalyzed hydrogen exchange, as well as an increased rate of apparent base-catalyzed hydrogen exchange, can be analyzed for the c-acetamide function. This apparent acidification of the c-acetamide function can be rationalized by the existence of a specific hydrogen bond involving its carbonyl oxygen.

In the case of primary amides, one also has to take into account intramolecular exchange (*E/Z* isomerization), which leads to a more complicated exchange dynamics. Careful inspection of the temperature dependence of the intra-amide ROESY or exchange peaks additionally supports hydrogen bonding of the c-side chain. A hydrogen bond, i.e., XH···O=C, induces polarization of the amide N–C bond, and this bond



exhibits more double-bond character and becomes shorter<sup>77</sup> and more rigid. Thus, for primary amides one would expect a reduced rate of intra-amide exchange, provided hydrogen bonding occurs. Indeed, at room temperature (26 °C), the two c-amide protons show only ROESY cross peaks and no chemical exchange, whereas the other amide protons exchange rapidly, apparently due to rotation around the C–N bond. At lower temperature (5 °C), ROESY cross peaks occur for all amide protons due to hindered rotation (see Figure 14).

The existence of the H-bond between the cobalt-coordinated water molecule and the c-acetamide carbonyl oxygen is also supported by arguments based upon <sup>15</sup>N chemical shifts, known to be sensitive to hydrogen bonding.<sup>75</sup> The effect is most pronounced when the carbonyl group interacts with proton donors, when a decrease in electron density on the amide nitrogen<sup>78a</sup> is accompanied by a low-field shift of the corresponding <sup>15</sup>N resonance.<sup>78</sup> We have investigated coenzyme B<sub>12</sub> and some of its derivatives and found that the amide <sup>15</sup>N chemical shifts are rather insensitive to variation of the organic ligand (in contrast to the corrin and DMB nitrogens). However, there is a significant downfield shift (by ca. 3 ppm) of the <sup>15</sup>N chemical shift of the c-acetamide nitrogen of 1<sup>+</sup>, compared to that of coenzyme B<sub>12</sub>, where such a hydrogen bond is unlikely to exist.<sup>79</sup>

The NMR data obtained for H<sub>2</sub>O solution of 1<sup>+</sup> are compatible with a solution structure of the aquocobalamin ion that has some of the same basic features as in the crystal structure, i.e., a cobalt-coordinated water that hydrogen bonds to the carbonyl oxygen (O39) of the c-acetamide chain, a close approach of the nucleotide base to the corrin ring, and an extended d-side chain. However, significant differences are indicated from qualitative NOE distance constraints with respect to the time-averaged conformation of the hydrogen-bonded c-acetamide chain and the e-propionamide side chain.

## Conclusions

In the present work, the structure of the aquocobalamin ion has been investigated at high accuracy in the crystal and in solution. As expected on the basis of arguments from coordination chemistry, an extremely short approach of the nucleotide base toward the cobalt–corrin moiety is indicated, resulting in remarkable steric strain between the two units. In this way, the basic mechanism of the mechanochemical effect of the nucleotide base on the cobalt–corrin moiety has been experimentally verified for a “nonalkyl” cobalamin. These results set the stage for structural correlations establishing a mechanical model for the response of the B<sub>12</sub> system to structural deformations.

## Experimental Section

**Preparation of Aquocobalamin Perchlorate Crystals Grown from Water.** “Aquocobalamin hydrochloride” (550 mg) from Roussel-UCLAF<sup>17</sup> was dissolved in 5 mL of distilled water; 3 g of solid sodium perchlorate, 0.5 mL of 0.1 M aqueous perchloric acid, and 10 mL of acetone were added. A crystalline precipitate formed from this deep red solution overnight in the cold room. It was separated from its mother liquor, washed with acetone, and dried (460 mg). This procedure was repeated once; 180 mg of the so-obtained dried

crystalline precipitate was dissolved in 4 mL of water at room temperature, and the solution was transferred to the refrigerator. Large crystals appeared after several days. Crystals from the same crystallization batch were used for the X-ray structure determination and for the EXAFS spectra of crystalline 1<sup>+</sup>ClO<sub>4</sub><sup>-</sup> (see below).

**X-ray Single-Crystal Structure Analysis of Aquocobalamin Perchlorate (1<sup>+</sup>ClO<sub>4</sub><sup>-</sup>).** A crystal of dimensions 0.4 × 0.45 × 0.8 mm was mounted in a 1 mm glass capillary. Room-temperature unit-cell parameters were obtained on a locally constructed four-circle diffractometer (Mo Kα radiation, graphite monochromator, λ = 0.71069 Å) by least-squares refinement against the setting angles of 35 reflections with 6° ≤ 2θ ≤ 15°. Crystals were orthorhombic, space group P2<sub>1</sub>2<sub>1</sub>2<sub>1</sub>, with four formula units (C<sub>62</sub>H<sub>90</sub>N<sub>13</sub>O<sub>15</sub>PCoClO<sub>4</sub>·25H<sub>2</sub>O, total formula weight 1897.2, 450.4 for solvent molecules) in the unit cell: a = 15.042(1) Å, b = 23.715(14) Å, c = 25.104(12) Å, V = 8955(2) Å<sup>3</sup>, d<sub>calc</sub> = 1.407 g/cm<sup>3</sup>, d<sub>obs</sub> = 1.356 g/cm<sup>3</sup> (determined by flotation from n-hexane/chloroform).

Intensity data were collected from the same crystal, using a MAR rotation camera with imaging plate detector. These experiments were performed on the X31 beam line of the EMBL at the Deutsches Elektronen Synchrotron (DESY) in Hamburg, FRG. Data were collected at ambient temperature (298 K) with a wavelength of 0.65 Å to a resolution of 0.8 Å (0 ≤ h ≤ 18, 0 ≤ k ≤ 29, 0 ≤ l ≤ 31, 2θ ≤ 48.6°), yielding 22 867 unique and 20 942 significant (I/σ(I) > 2) reflections. Friedel-equivalent reflections were not merged. Data were corrected for Lorentz polarization but not for absorption (μ = 0.27 mm<sup>-1</sup>).

The structure of 1<sup>+</sup>ClO<sub>4</sub><sup>-</sup> was solved by locating the cobalt atom from a Patterson synthesis and then locating the lighter atoms in subsequent electron density maps. Atomic positions and isotropic and anisotropic (see below) atomic displacement parameters (adp's) were refined with a full-matrix least-squares program<sup>80</sup> which minimized the quantity Σw(F<sub>o</sub><sup>2</sup> - F<sub>c</sub><sup>2</sup>)<sup>2</sup> with w = 1/[σ<sup>2</sup>(F<sub>o</sub><sup>2</sup>) + (0.1P)<sup>2</sup> + 0.9P], P = (max(F<sub>o</sub><sup>2</sup>, 0) + 2F<sub>c</sub><sup>2</sup>)/3, using all reflections. Scattering factors including real and imaginary dispersion corrections were taken from ref 81.

Anisotropic adp's were refined for all non-hydrogen atoms of the cobalamin moiety, applying a “rigid bond” restraint<sup>82</sup> (effective standard deviation σ = 0.01 Å<sup>2</sup>) for all 1,2- and 1,3-distances. Hydrogen atom positions were calculated and refined as “riding” on their respective non-hydrogen atom. Methyl torsion angles were chosen to maximize the electron density at the three calculated H atom positions and allowed to refine. An analogous procedure was applied to the two ribose hydroxyl groups. The (isotropic) adp's for the hydrogen atoms were set to 1.5 times the equivalent isotropic adp of the adjacent non-H atom. Chemically equivalent bond lengths and 1,3-distances of the amide side chains were restrained to be equal; the atoms of the amide groups and the imidazole base were restrained to be coplanar. The two protons of the Co-coordinated water molecule were located in a difference electron density map (see Figure 4) and allowed to refine subject to appropriate distance restraints (d(O - H) = 0.95(1) Å, d(H - H) = 1.56(3) Å).

The solvent electron density was modeled by including 25 water molecules, whose oxygen atoms were refined with anisotropic adp's and unit occupancy. Eleven solvent hydrogen atoms were located in difference electron density maps and refined with the above O–H and H–H distance restraints.

Refinement of 1165 parameters against 22 867 intensity data and 649 restraints converged at the following values for the reliability indices: wR<sub>2</sub> = [Σ[w(F<sub>o</sub><sup>2</sup> - F<sub>c</sub><sup>2</sup>)<sup>2</sup>]/Σ[w(F<sub>o</sub><sup>2</sup>)<sup>2</sup>]<sup>1/2</sup> = 0.1289 (for all 22 867 reflections), R<sub>1</sub> = Σ|F<sub>o</sub> - |F<sub>c</sub>||/Σ|F<sub>o</sub>| = 0.045 for 20 942 reflections with F<sub>o</sub> > 4σ(F<sub>o</sub>) and 0.050 for all 22 867 data; goodness-of-fit S = [Σ[w(F<sub>o</sub><sup>2</sup> - F<sub>c</sub><sup>2</sup>)<sup>2</sup>]/[n - p]<sup>1/2</sup> = 1.033 (n = 22 867, number of observations; p = 1165, number of parameters). Features up to 0.47(6) eÅ<sup>-3</sup> and down to -0.47(6) eÅ<sup>-3</sup> were observed in a final difference electron density map. The absolute structure parameter<sup>83</sup>

(77) Jeffrey, G. A.; Saenger, W. *Hydrogen bonding in Biological Structures*, 2nd printing; Springer: Berlin, Heidelberg, 1994.

(78) (a) Saito, H.; Tanaka, Y.; Nukada, K. *J. Am. Chem. Soc.* **1971**, *93*, 1077. (b) Kamlet, M. J.; Dickinson, C.; Taft, R. W. *J. Chem. Soc., Perkin Trans. 2* **1981**, 353. (c) Marchal, J. P.; Canet, D. *Org. Magn. Reson.* **1981**, *15*, 244. (d) Burgar, M. I.; St. Amour, T. E.; Fiat, D. *J. Phys. Chem.* **1981**, *85*, 502.

(79) Puchberger, M.; Maynollos, J.; Konrat, R.; Kräutler, B.; Kratky, C. To be submitted to *J. Am. Chem. Soc.*

(80) (a) Sheldrick, G. M. SHELXL-93, a program for the refinement of crystal structures from diffraction data, University of Göttingen, 1993. (b) SHELXTL-PC, Release 4.1, Siemens Crystallographic Research Systems, 1990.

(81) *International Tables for Crystallography*; Wilson, A. J. C., Ed.; Kluwer Academic Publishers: Dordrecht, 1992; Vol. C.

(82) Hirshfeld, F. L. *Acta Crystallogr. A* **1976**, *32*, 239.

(83) Flack, H. D. *Acta Crystallogr. A* **1983**, *39*, 876.

converged to 0.013(8) (a value of 0 indicating the correct enantiomer and a value of 1 the opposite enantiomer).

The atomic numbering used for the description of the structure is defined in Figure 1. Fractional coordinates of the non-hydrogen atoms are given together with their equivalent isotropic adp's in Table S2; anisotropic adp's of these atoms, fractional coordinates for hydrogen atoms, comprehensive tables with the molecular geometry, and a table of hydrogen bond lengths are given in Tables S5, S6, S3, and S4, respectively. All these tables have been included in the supplementary material. The coordinates have also been deposited with the Cambridge Structural Data Base.

**EXAFS Spectra of Aquocobalamin Perchlorate ( $I^+ClO_4^-$ ) in Solution and in the Solid State.** Hydroxocobalamin hydrochloride (396 mg) (Sigma Chemical Co.) was dissolved in 10 mL of doubly distilled H<sub>2</sub>O and treated with 60  $\mu$ L of distilled triethylamine (1.5 equiv). The dark red precipitate which occurred on adding an excess of acetone was filtered, washed with pure acetone, and dried, yielding 361 mg (93%) of a dark red precipitate, identified as hydroxocobalamin (5) by X-ray analysis of a recrystallized sample.<sup>63</sup> The absence of chloride ions was tested using a solution of AgNO<sub>3</sub> in water.

For the solution spectra a concentrated solution of 5 in water/ethylene glycol (1:1) was prepared and an excess of HClO<sub>4</sub> was added. This solution was injected into a 1 mm cell. The concentration (118 mM) and the identity of I<sup>+</sup> were determined by optical spectroscopy.

Solid-state X-ray absorption spectra were taken using crystals from the batch prepared for the X-ray structure determination (see above). Crystals were removed from their mother liquor, put on a strip of filter paper to remove adhering solution, and quickly covered with about twice their volume of a 1:2 mixture of paraffine oil and vacuum grease to prevent evaporation of internal solvent molecules from the crystal. The oil-covered crystals were crushed with a small spatula, and the slurry was packed into a 1 mm sample holder. Both the slurry and the solution were cooled to about 100 K by plunging into liquid nitrogen immediately after preparation.

Following the X-ray absorption measurements, the samples were warmed up to room temperature and UV/vis spectra were recorded. They did not indicate any radiation damage. Crystallinity of the solid sample was verified by taking a powder diffraction pattern after warming up.

X-ray absorption spectra at the Co K edge (approximately 7717 eV) of I<sup>+</sup>ClO<sub>4</sub><sup>-</sup> (both solution and crystalline sample) were recorded in the absorption mode at the EMBL EXAFS station at DESY in Hamburg. The major components of the beam line include an order sorting Si(111) monochromator, a segmented, focusing Au-coated mirror, and an energy calibration device.<sup>84</sup> For harmonic rejection, the monochromator was detuned to 70% of its peak intensity. The energy resolution of the spectrometer was 2.0 eV as established from the full width at half-maximum of the calibration Bragg peaks. During the experiments, the samples were located in the He exchange gas atmosphere (20 K) of a closed-cycle cryostat. *I* and *I*<sub>0</sub> were measured in the range from 7300 to 8700 eV using two ion chambers located in front of and behind the sample holder. All measurements were carried out during dedicated synchrotron radiation shifts with DORIS II instrument working at an energy of 4.48 GeV and a current of 80–30 mA.

The scans were repeated several times for solution and crystals,<sup>27</sup> every scan was individually energy calibrated, and five corresponding scans for each sample were averaged. A Victoreen-like function was used for the pre-edge fit; the isolated atom background was subtracted by fitting cubic splines (three to four segments) to the data from 20 to 800 eV. The resulting spectra were weighted by *k*<sup>3</sup>. For both cases, *E*<sub>0</sub> was set to 7717 eV. Data reduction was carried out with computer programs developed at the EMBL outstation.<sup>85</sup>

**NMR Experiments.** All NMR experiments were carried out on a Varian 500 Unity plus spectrometer with a 5 mm indirect detection probe equipped with gradient facilities. Experiments aimed at the elucidation or verification of spectral assignments were carried out with

10 mM solutions of aquocobalamin chloride (I<sup>+</sup>Cl<sup>-</sup>) in 100 mM phosphate buffer, pH 3.5, sample size 0.7 mL, 26 °C.

**Gradient-Enhanced Heteronuclear Single-Quantum Coherence Experiment (PFG-HSQC).**<sup>32,33</sup> Two sets of spectra were recorded and processed according to the STATES<sup>86</sup> recipe to yield a pure absorption spectrum with quadrature in *F*<sub>1</sub>. The one-bond <sup>1</sup>H-<sup>13</sup>C shift correlation spectra of aquocobalamin resulted from a 2 × 256 × 1024 data matrix size, with four scans per *t*<sub>1</sub> value and a delay time between scans of 1 s. The first gradient was applied with a strength of 19.75 G/cm and a duration of 2 ms, while the second gradient pulse of 19.48 G/cm was applied for 0.5 ms. The one-bond <sup>1</sup>H-<sup>15</sup>N shift correlation spectra resulted from a 2 × 128 × 1024 data matrix size, with 32 scans per *t*<sub>1</sub> value and a delay time between scans of 1 s. The first gradient was applied with a strength of 27.5 G/cm and a duration of 2.5 ms, while the second gradient pulse of 13.7 G/cm was applied for 0.5 ms. All gradients were rectangular and applied along the *z*-axis. Decoupling (during acquisition) was achieved with the use of the GARP decoupling sequence,<sup>87</sup> using a 3.7 and 1.5 kHz radio frequency field for the <sup>13</sup>C and the <sup>15</sup>N correlation spectra, respectively. Shifted squared sine-bell windows were used both in *t*<sub>1</sub> and *t*<sub>2</sub>. Low-frequency subtraction in the time domain was applied to improve the spectra, using standard Varian Vnmr software (lfs).

**Gradient-Enhanced <sup>1</sup>H-Detected Multiple-Bond Heteronuclear Multiple-Quantum Coherence Experiment (PFG-HMBC).**<sup>32,34</sup> Magnitude mode spectra were obtained using the standard gradient-enhanced HMQC pulse sequence with an additional delay for the evolution of the long range heteronuclear coupling. The multiple-bond <sup>1</sup>H-<sup>13</sup>C shift correlation spectrum resulted from a 512 × 1024 data matrix size, with 16 scans per *t*<sub>1</sub> value and a delay time between scans of 1 s. The first two gradients were applied with strengths of 9.87 G/cm each, while the third gradient pulse had a strength of 4.98 G/cm. The multiple-bond <sup>1</sup>H-<sup>15</sup>N shift correlation spectrum resulted from a 512 × 1024 data matrix size, with 200 scans per *t*<sub>1</sub> value and a delay time between scans of 1 s. The first two gradients were applied with strengths of 18.4 G/cm, while the third gradient pulse had a strength of 3.7 G/cm. The durations of the three gradient pulses were 2 ms. All gradients were rectangular and applied along the *z*-axis. Shifted squared sine-bell windows were used prior to Fourier transformation in both *t*<sub>1</sub> and *t*<sub>2</sub>.

**Band-Selective Pulsed Field Gradient Heteronuclear Multiple-Bond Correlation Spectroscopy (PFG-HMBC).**<sup>30,32,34</sup> Magnitude mode spectra were obtained using the standard gradient-enhanced HMBC pulse sequence using a EBURP-2<sup>88</sup> band-selective excitation pulse for the excitation of the carbon region of interest. The selective multiple-bond <sup>1</sup>H-<sup>13</sup>C shift correlation spectrum of Figure S8 (supplementary material) resulted from a 128 × 1024 data matrix size, with 32 scans per *t*<sub>1</sub> value and a delay time between scans of 1 s. Band-selective excitation of the carbon region was obtained with a 4 ms EBURP-2<sup>88</sup> excitation pulse. The first two gradients were applied with strengths of 9.876 G/cm each, and the third gradient pulse had a strength of 4.98 G/cm. The durations of the three gradient pulses were 2 ms. All gradients were rectangular and applied along the *z*-axis. Shifted squared sine-bell windows were used prior to Fourier transformation in both *t*<sub>1</sub> and *t*<sub>2</sub>.

**"Watergate" Total Correlation Spectroscopy.**<sup>89,68</sup> The TOCSY spectrum resulted from a 512 × 1024 data matrix with eight scans per *t*<sub>1</sub> value. Delay between experiments was 1 s. Pulse length for selective excitation of the water signal in the watergate step was 4.3 ms. Gradient strengths were as follows: 12 G/cm, 3 ms (during the Z-filter); -12 G/cm, 1 ms (during the watergate period). A DIPSY<sup>90</sup> mixing sequence of 75 ms preceded by a 2.0 ms trim pulse was used. A 7.8 kHz rf field strength (corresponding to a 32  $\mu$ s 90° <sup>1</sup>H pulse width) was used.

(86) States, D. I.; Haberkorn, R. A.; Ruben, D. J. *J. Magn. Reson.* **1982**, *48*, 286.

(87) Shaka, A. J.; Barker, P. B.; Freeman, R. *J. Magn. Reson.* **1985**, *64*, 547.

(88) Geen, H.; Freeman, R. *J. Magn. Reson.* **1990**, *87*, 415.

(89) (a) Braunschweiler, L.; Ernst, R. R. *J. Magn. Reson.* **1983**, *53*, 521. (b) Bax, A.; Davies, D. G. *J. Magn. Reson.* **1985**, *65*, 355. (c) Davies, D. G.; Bax, A. *J. Am. Chem. Soc.* **1985**, *107*, 2820.

(90) Shaka, A. J.; Lee, C. J.; Pines, A. *J. Magn. Reson.* **1988**, *77*, 274.

(84) (a) Hermes, C.; Gilberg, E.; Koch, M. H. J. *Nucl. Instrum. Methods* **1984**, *222*, 207. (b) Pettifer, R. F.; Hermes, C. *J. Appl. Crystallogr.* **1985**, *18*, 404. (c) Pettifer, R. F.; Hermes, C. *J. Phys. (Paris)* **1986**, *47*, 127.

(85) Nolting, H.-F.; Hermes, C. *EXPROG: EMBL-EXAFS data analysis and evaluation program for PC/AT*; European Molecular Biology Laboratory: Hamburg, 1992.



A cosine-bell squared filter was used in both  $t_1$  and  $t_2$  dimensions. Quadrature detection in  $F_1$  was achieved by means of the STATES recipe.<sup>86</sup>

**“Watergate” Spin-Locked NOE Spectroscopy (“Watergate” ROESY).**<sup>91,68,3\*</sup> The ROESY spectrum of aquocobalamin resulted from a  $512 \times 1024$  data matrix before and  $1K \times 2K$  after zero-filling, with 16 scans per  $t_1$  value. Predelay was 1 s, and the mixing time was 200 ms. A 3.1 kHz rf field strength was used. Gradient strengths and durations were as follows: G0, 20 G/cm, 4 ms; G1, -5 G/cm, 0.8 ms; G2, 5 G/cm, 2 ms. Cosine-bell squared filters were used in both  $t_1$  and  $t_2$  dimensions. Standard Varian Vnmr solvent suppression (zfs) and base line correction routines (bc) were used. Quadrature detection in  $F_1$  was achieved by means of the STATES recipe.<sup>86</sup>

**SS-NOESY.**<sup>67</sup> The NOESY spectrum of  $1^+Cl^-$  resulted from a  $512 \times 1024$  data matrix before and  $1K \times 2K$  after zero-filling, with 16 scans per  $t_1$  value. Predelay was 1 s, and the mixing time was 400 ms. A laminar shifted  $90^\circ$  SS excitation pulse<sup>92</sup> with a  $333.8 \mu s$  duration was calculated, effective rf field of 1.5 kHz. Cosine-bell squared filters were used in both  $t_1$  and  $t_2$  dimensions. Standard Varian Vnmr solvent suppression (zfs) and base line correction routines (bc) were used. To remove first-order base line roll, the FID was shifted to the right by one data point, which was subsequently back-predicted by linear prediction. Quadrature detection in  $F_1$  was achieved by means of the STATES recipe.<sup>86</sup>

**Measurement of Rates of Proton Exchange with Solvent Water.** Solutions (0.7 mL) of  $1^+Cl^-$  had a concentration of 1 mM in 10 mM phosphate buffer, with pH values of 1.6, 1.9, 3.0, 3.5, 4.0, 5.0, 6.6, and 9.3. Data regarding the presence of hydrogen bonds were acquired from 1D experiments recorded with and without presaturation, as described in ref 93.

(91) (a) Bothner-By, A. A.; Stephens, R. L.; Warren, C. D.; Jeanloz, R. W. *J. Am. Chem. Soc.* **1984**, *106*, 811. (b) Bax, A.; Davies, D. G. *J. Magn. Reson.* **1985**, *63*, 207.

(92) Patt, S. L. *J. Magn. Reson.* **1992**, *96*, 94.

**Acknowledgment.** C.K., G.F., K.G., and B.K. acknowledge support by the Österreichischer Fonds zur Förderung der Wissenschaftlichen Forschung (Projects Nr. 8371 (C.K. and G.F.), 9334 (B.K.), and 9542 (C.K. and K.G.)) and the Jubiläumsfonds der Österreichischen Nationalbank (Proj. Nr. 4991 (C.K. and K.G.)). We thank T. Dérer for preparation of aquocobalamin samples for NMR spectroscopy.

**Supplementary Material Available:** Tables S1–S6 with results from the crystal structure analysis of aquocobalamin perchlorate ( $1^+ClO_4^-$ ) including general crystal data, fractional atomic coordinates, bond lengths, bond angles, and torsion angles, intra- and intermolecular hydrogen bond distances, anisotropic atomic displacement parameters, and calculated positions of hydrogen atoms, EXAFS spectrum of crystalline aquocobalamin perchlorate ( $1^+ClO_4^-$ ) (Figure S7), and Figures S8 and S9 with NMR data from  $1^+Cl^-$  including band-selective pulsed field gradient heteronuclear multiple-bond correlation spectrum (BS PFG-HMBC) and contour plot of the 200 ms “watergate” ROESY (23 pages). This material is contained in many libraries on microfiche, immediately follows this article in the microfilm version of the journal, can be ordered from ACS, and can be downloaded from the Internet; see any current masthead page for ordering information and Internet access instructions.

JA944203X

(93) (a) Waelder, S.; Redfield, A. G. *Biopolymers* **1977**, *16*, 623. (b) Rosevaer, P. R.; Fry, D. C.; Mildvan, A. S. *J. Magn. Reson.* **1985**, *61*, 102. (c) Krishna, N. R.; Huang, D. H.; Glickson, J. D.; Rowan, R.; Walter, R. *Biophys. J.* **1979**, *26*, 345. (d) Spera, S.; Ikura, M.; Bax, A. *J. Biomol. NMR* **1991**, *1*, 155.